

Dissertation

presented to obtain the

HABILITATION À DIRIGER DES RECHERCHES

Université Paul Sabatier Toulouse 3

Mention: Applied Mathematics

by

Luc MIEUSSENS

**Contributions to the numerical simulation in Kinetic Theory:
implicit schemes, coupling of models,
asymptotic models.**

Defended on 13 December 2007

After reviews by:

A. KLAR, Professor	Technische Universität Kaiserslautern
F. GOLSE, Professor	École Polytechnique
E. SONNENDRÜCKER, Professor	Université Louis Pasteur, Strasbourg

Committee Members:

F. BOUCHUT, Research Director	CNRS and École Normale Supérieure
Y. BRENIER, Research Director	CNRS and Université de Nice-Sophia-Antipolis
P. CHARRIER, Professor	Université Bordeaux 1
P. DEGOND, Research Director	CNRS and Université Paul Sabatier Toulouse 3
F. GOLSE, Professor	École Polytechnique
E. SONNENDRÜCKER, Professor	Université Louis Pasteur, Strasbourg

Contents

Introduction	5
1 Time implicit schemes for the Landau equation [1, 2, 3]	9
1.1 Time implicit schemes for the space homogeneous Landau equation	10
1.2 Linear solvers	13
1.3 Application to the isotropic Landau equation	15
1.4 Perspectives	15
2 Coupling kinetic and fluid models	17
2.1 Kinetic/fluid coupling by domain decomposition without interface boundary condition [4]	18
2.2 Kinetic/fluid coupling with a moving interface [5]	24
2.3 Fluid model with local kinetic upscalings [6]	26
2.4 Perspectives	29
3 Asymptotic preserving numerical methods for kinetic equations in the fluid limit	31
3.1 Numerical scheme for the Boltzmann equation preserving the compressible Navier-Stokes asymptotics [7]	32
3.2 A numerical scheme for the linear transport equation preserving the diffusion asymptotics [8]	36
3.3 Perspectives	39
4 Models and numerical computations for a problem of microfluidics	41
4.1 Thermal creep flow and Knudsen compressors	41
4.2 Two-dimensional steady Boltzmann-BGK simulation with an implicit scheme [9, 10]	44
4.3 Diffusion approximation induced by the collisions with the boundaries [11, 12]	48
4.4 Approximation by a hydrodynamic model [13]	53
4.5 Perspectives	53
5 Construction and comparisons of some simplified kinetic models	55
5.1 Velocity discretization of a BGK model for the polyatomic gases [14]	55
5.2 Construction and numerical approximation of BGK models with velocity dependent collision frequency [15, 16]	58

5.3 Numerical comparison for a kinetic equation and two Spherical Harmonics	
Expansion models [17]	59
Publications	63
Bibliography	65

Introduction

The numerical simulation of particle systems as described by the kinetic theory is used in various fields: let us mention, for instance, rarefied gas dynamics, neutron transport, and radiative transfer. Many researchers in numerical analysis and scientific computing have been working on these fields for a long time. Nowadays, the kinetic theory is applied to new fields as population dynamics or vehicular traffic: these fields also require researches in numerical simulation.

The main difficulty presented by these simulation problems is the large complexity of the underlying mathematical models: they are often integro-differential equations with a large number of variables. For instance, many problems in the kinetic theory of gases contain one time variable, three space variables, and three velocity variables, while there are even more complex cases (polyatomic molecules, multi-species gases, variable size particles, etc.). Furthermore, there is another kind of difficulty: kinetic problems often contain very different time and space scales. For instance, for photon transport in a heterogenous medium, the time scale may have large variations depending on the opacity of the medium. In the equations, these different scales generate stiff terms that induce very strong constraints on the numerical parameters.

Such difficulties require to design efficient numerical methods so that modern computers can make accurate simulations for a reasonable computational time. Of course, many approaches have been proposed: generally speaking, they are all based on techniques of acceleration of the kinetic computations by suitable algorithms, or on simplifications of the physical model. It is important to mention that all these approaches are linked together: many of them can make use of an improvement of some others. Let us give below a non exhaustive list of these different approaches.

Generally, the simplification of a kinetic model is based on the following idea: in regimes where there are numerous collisions, the system is close to an equilibrium state, and the kinetic model can be replaced by a macroscopic model, which is much simpler to solve numerically. This is how are obtained the classical equations of fluid mechanics or the diffusion equations of linear transport and radiative transfer. There are also some methods to extend the validity domain of the macroscopic models to the regions where the system is less close to the equilibrium (higher order asymptotic models, moment models, boundary layer corrections). This is still a very active field, in particular with the recent researches in microfluidics or in plasma physics.

When there are different scales in different zones of the computational domain, it is natural to speed up the simulation by using the kinetic and macroscopic models in their

respective validity domains. The difficulty is here to identify the different domains, and to find a way to correctly match the two descriptions. If the transition between the two domains is not localized enough, either the macroscopic model is required to be extended beyond the equilibrium regime (this has been mentioned above), or the kinetic solving must be efficient enough in near equilibrium zones.

This last constraint is taken into account by the “Asymptotic Preserving” (AP) scheme theory. The goal is here to design methods that are stable and accurate, uniformly with respect to the scaling parameters of the problem. To obtain the uniform stability, in particular the time stability, an essential tool is the time implicit discretization. This is a technique which is known to somehow “filter” the fast time variations, and which is used, for instance, for equations with stiff source terms (like in case of numerous collisions) or for diffusion equations (where the stiffness is due to high frequencies). However, this technique requires to solve very large linear or nonlinear systems. This may be why it was used only recently in kinetic theory, while it has been used for a long time in Computational Fluid Dynamics, for instance. Due to recent advances in matrix numerical analysis (sparse linear solvers, Newton-Krylov methods, etc.), it is now possible to efficiently make use of these implicit techniques.

Finally, we mention the problem of efficient algorithms for collision computations. This is mainly important for nonlinear problems like the Boltzmann equation where the particles collide each others. The goal is then to obtain algorithms that are fast (their complexity should be proportional to the number of particles) and that preserve the physical properties (like conservation and entropy properties). Various methods, that are still the subject of investigations, give more or less satisfying results: probabilistic methods like the Direct Simulation Monte Carlo, or deterministic methods like multigrid or spectral approaches. Another possibility, much simpler, consists in modifying the collision operator, generally by using a relaxation model.

This report gathers the results I have obtained, in collaboration with various people, in the different fields mentioned above. Almost all those works contain new simulation methods for the kinetic theory, and their potentialities are illustrated by various numerical tests. The proposed approximations are sometimes justified by mathematical results (stability, preservation of conservation and entropy properties), but the rigorous mathematical analysis of these methods is a wide project that is still to be investigated. Chapter 1 is devoted to new implicit schemes for the Landau equation. This kinetic equation contains a diffusion-like source term that induced a spectral stiffness. We study the possibility to design implicit schemes that yield fast and conservative methods. In chapter 2, we present two new coupling methods in which the idea is to avoid the interface boundary condition. The second method is a rather general multiscale approach which takes the kinetic description into account so as to locally refine a macroscopic model. This idea is also used in chapter 3 to develop AP schemes: it allows to discretize differently the different scales of the problem to obtain very efficient schemes. Chapter 4 gathers several results for the numerical simulation of a new micropump system. We have proposed different techniques (deterministic kinetic simulations, macroscopic modeling by a diffusion approximation) and have used existing techniques (DSMC, compressible Navier-Stokes equations). Finally, chapter 5 contains more

independent works devoted to some simplified models like the BGK model (construction and discretization) and the SHE model (numerical comparisons).

To close this introduction, I specify a few facts about the presentation of this report. Numerical citations like [1], [2], etc., refer to the list of my publications given page 63. The other references like [CBKM00] refer to the general bibliography given page 65. To preserve a kind of homogeneity, the notations used in this document are sometimes different from these used in the corresponding articles. Finally, each section ends with a few numerical results given to illustrate the properties of the method, but note that the corresponding articles contain various other results.

Chapter 1

Time implicit schemes for the Landau equation [1, 2, 3]

The Fokker-Planck-Landau equation (FPL) is a kinetic equation that models particle systems in plasma physics. The main numerical difficulty of this equation is that the collision operator contains diffusion terms with respect to the velocity variable. Consequently, the space homogeneous FPL equation (which is considered in the standard time splitting scheme, for instance) is nothing but a convection-diffusion equation with non-local coefficients. Any time discretization of this equation must then face the classical problem of the numerical stability of approximations of diffusion equations. Usually, this kind of equations is discretized with a time implicit scheme, which remove the stiffness induced by the diffusion. However, because of the complexity of the FPL equation, using implicit schemes is rather difficult, and has been studied only quite recently.

In this chapter, we summarize the results obtained in collaboration with M. Lemou and published in the *SIAM Journal of Scientific Computing* in 2005 [2] (see also Note [1] and a slightly extended version in proceedings [3]). In section 1.1, we propose several new time numerical schemes for which we try to combine the implicit time discretization with the following two properties

- preservation of the conservation properties: we guarantee these properties, even if our schemes contain linear systems that are solved by iterative linear solvers only approximatively (section 1.2);
- fast algorithms: by using the entropy property, we construct symmetric methods that allow to use fast linear solvers like the Conjugate Gradient.

These schemes are applied to the isotropic FPL equation in section 1.3. Finally, we give some perspectives for the three-dimensional case in section 1.4.

Note that we do not consider here the problem of the velocity discretization: we use existing methods, even if this subject is worth to be developed.

1.1 Time implicit schemes for the space homogeneous Landau equation

The space homogeneous FPL equation is written in the Landau form

$$\partial_t f(t, v) = Q(f)(v) = \nabla \cdot \int_{\mathbb{R}^d} \Phi(v - v_*) (f(v_*) \nabla f(v) - f(v) \nabla f(v_*)) dv_*, \quad (1.1)$$

where f is the distribution function of particle velocities, that depends on time t and velocity $v \in \mathbb{R}^d$ ($d = 2, 3$). The kernel $\Phi(w)$ is the following $d \times d$ matrix:

$$\Phi(w) = C|w|^{\gamma+2} S(w) = C|w|^{\gamma+2} \left(I_d - \frac{w \otimes w}{|w|^2} \right).$$

In this expression, C is a positive constant and γ is a parameter leading to the standard classification in hard potentials ($\gamma > 0$), Maxwellian potential ($\gamma = 0$) and soft potentials ($\gamma < 0$). This last case includes the most physically interesting case, the Coulombian case ($\gamma = -3$). The $d \times d$ matrix $S(w)$ is simply the orthogonal projection onto the plane orthogonal to w . For all $w \neq 0$, $\Phi(w)$ is a positive matrix whose null-space is $\text{Ker } \Phi(w) = \mathbb{R}w$. It is also useful to write the collision operator $Q(f)$ under the following equivalent form (called ‘‘Log’’ form)

$$Q(f)(v) = \nabla \cdot \int_{\mathbb{R}^d} \Phi(v - v_*) f(v) f(v_*) (\nabla \log f(v) - \nabla \log f(v_*)) dv_*. \quad (1.2)$$

With this formulation, we can easily prove the conservation and entropy properties: for every positive g , we have

$$\int_{\mathbb{R}^d} (1, v, \frac{1}{2}|v|^2) Q(g) dv = 0 \quad \text{and} \quad \int_{\mathbb{R}^d} Q(g) \log(g) dv \leq 0.$$

The previous inequality implies that for the solution f of (1.1), the entropy $H(f) = \int f \log f dv$ is a non-increasing function of t , while the quantities $\int (1, v, \frac{1}{2}|v|^2) f dv$ are constant. Moreover, this inequality becomes an equality if and only if f is a Maxwellian

$$f_{eq}(v) = \frac{\rho}{(2\pi T)^{\frac{d}{2}}} \exp\left(-\frac{|v - u|^2}{2T}\right), \quad (1.3)$$

where ρ, u and T are parameters independent of the velocity. This is formally equivalent to the fact that f is an equilibrium state, that is to say $Q(f) = 0$.

Note that equation (1.1) is a convection-diffusion equation that can be written under the form

$$\partial_t f = \nabla \cdot (D(f) \nabla f + F(f) f), \quad (1.4)$$

where $D(f) = \int_{\mathbb{R}^d} \Phi(v - v_*) f(v_*) dv_*$ and $F(f) = \int_{\mathbb{R}^d} \Phi(v - v_*) \nabla f(v_*) dv_*$. It can then be expected that for an explicit time discretization of this equation (like the simple backward Euler), the time step must be satisfy a stability constraint of type $\Delta t = O(\Delta v^2)$, where Δv is the velocity discretization step. Of course, this is prohibitive, in terms of computational

cost, when Δv is small. Usually, when time implicit schemes are used, such constraints disappear, since implicit schemes are uniformly stable with respect to the mesh size.

However, one must satisfy several severe constraints to obtain an efficient implicit scheme. For instance, it is essential that the numerical method satisfies the properties of conservation and entropy. Moreover, it is necessary to use fast linear solvers to insure that the implicit method is faster than a simple explicit scheme.

To illustrate the difficulty of this problem, we cite the outstanding work of Chacón, Barnes, Knoll and Miley [CBKM00] who use the diffusion form (1.4) and compute the coefficients D and F by the Rosenbluth method: in the Coulombian case, these coefficients are written with Poisson integrals that can be efficiently computed by a fast Poisson solver. This makes their method very fast, but the conservation and entropy properties are not preserved. This implies that a thin enough velocity discretization has to be used so as to avoid too many numerical errors.

In this work, we have proposed to use the Landau form (1.1) or the “Log” form (1.2), in order to obtain implicit schemes that naturally satisfy the conservation properties, and for some of them, the entropy property (which is much more difficult to obtain). Moreover, most of our schemes are linear, in order to obtain fast computations. We rapidly describe below these different schemes and their properties (see [2] for details). As it is usual, f^n denotes, in the following, an approximation of the distribution f at time $t_n = n\Delta t$, where Δt is a given time step.

A first class of numerical schemes is obtained by using linearized forms of the operator Q written on the Landau form. Namely, the bilinear products are approximated so that only one term of the product is evaluated at time t_{n+1} . This linearization preserves the symmetries that induce the conservation properties. Our schemes are the followings.

contracted scheme:

$$\frac{f^{n+1} - f^n}{\Delta t} = q^c(f^n, f^{n+1}), \quad \text{with} \quad (1.5)$$

$$q^c(f, g) = \nabla \cdot \int_{\mathbb{R}^d} \Phi(v - v_*) (f_* \nabla g - f \nabla g_*) dv_*, \quad (1.6)$$

where we note $f_* = f(v_*)$ and $f = f(v)$. This scheme is first order in time, and is conservative.

θ -scheme:

$$\frac{f^{n+1} - f^n}{\Delta t} = Q(f^n) + \theta q(f^n, f^{n+1} - f^n), \quad (1.7)$$

where $\theta \in \mathbb{R}$ and $q(f, \cdot)$ is the linearized of Q at f , given by

$$\begin{aligned} q(f, g) &= \nabla \cdot \int_{\mathbb{R}^d} \Phi(v - v_*) (f_* \nabla g - f \nabla g_* + g_* \nabla f - g \nabla f_*) dv_* \\ &= q^c(f, g) + q^c(g, f). \end{aligned} \quad (1.8)$$

This scheme is second order in time for $\theta = \frac{1}{2}$, and first order for other values of θ . It is conservative.

For these two schemes, we cannot prove the entropy property. Then we propose another class of schemes, based on the ‘‘Log’’ form (1.2). Our first scheme, which is nonlinear, is

log scheme:

$$\frac{f^{n+1} - f^n}{\Delta t} = q^{\log}(f^n, f^{n+1}) = \nabla \cdot \int_{\mathbb{R}^d} \Phi(v - v_*) f^n f_*^n (\nabla \log f^{n+1} - \nabla \log f_*^{n+1}) dv_*. \quad (1.9)$$

This scheme is first order in time, conservative, and has a non-increasing entropy. To obtain a linear scheme, the logarithm in q^{\log} is linearized, which yields the

log-linear scheme:

$$\frac{f^{n+1} - f^n}{\Delta t} = Q(f^n) + q^l(f^n, f^{n+1} - f^n), \quad \text{with} \quad (1.10)$$

$$q^l(f, g) = \nabla \cdot \int_{\mathbb{R}^d} \Phi(v - v_*) f f_* \left(\nabla \left(\frac{g}{f} \right) - \nabla \left(\frac{g}{f} \right)_* \right) dv_*. \quad (1.11)$$

This scheme is first order in time and conservative. It has very strong properties, like the entropy decay and a symmetry property, as it is stated in the following proposition

Proposition 1.1. (i) *Weak form of q^l :*

$$\begin{aligned} & \int_{\mathbb{R}^d} q^l(f, g) \phi dv \\ &= -\frac{1}{2} \int_{\mathbb{R}^d} \int_{\mathbb{R}^d} \Phi(v - v_*) f f_* \left(\nabla \left(\frac{g}{f} \right) - \nabla \left(\frac{g}{f} \right)_* \right) \cdot (\nabla \phi - \nabla \phi_*) dv dv_*. \end{aligned} \quad (1.12)$$

(ii) *The collisional part of scheme (1.10) dissipates an entropy, in the following sense:*

$$\int_{\mathbb{R}^d} (Q(f) + q^l(f, g)) \left(\log f + \frac{g}{f} \right) dv \leq 0.$$

(iii) *Discrete H-theorem: the entropy sequence $H_n = \int_{\mathbb{R}^d} f^n \log f^n dv$ is non-increasing if*

$$\inf_{n \in \mathbb{N}, v \in \mathbb{R}^d} \left(\frac{f^{n+1}}{f^n} \right) \geq \frac{1}{2}. \quad (1.13)$$

(iv) *For every positive f , the linear operator $g \mapsto q^l(f, g)$ is self-adjoint non-positive, in the following sense:*

$$\langle q^l(f, g), h \rangle_{\frac{1}{f}} := \int_{\mathbb{R}^d} q^l(f, g) h \frac{dv}{f} = \langle q^l(f, h), g \rangle_{\frac{1}{f}}, \quad \text{and} \quad \langle q^l(f, g), g \rangle_{\frac{1}{f}} \leq 0,$$

for every g and h .

This proposition can be proved by classical arguments: integration by parts, symmetry between v and v_* , convexity.

Note that property (iv) is very important, at the algorithmic level, since it allows to compute f^{n+1} by using the *Conjugate Gradient* solver, provided that the weight f^n used in the definition of the inner product is positive. This property is remarkable, since the FPL equation contains convection terms that generally do not lead to symmetric linear systems. For instance, the method of [CBKM00] has no symmetry property and cannot make use of the Conjugate Gradient.

However, it is not possible to guarantee that the weight f^n remains positive. Consequently, from the algorithmic point of view, none of the first two classes of schemes are completely satisfying. Then, we propose a third class of schemes based on the use of the Maxwellian equilibrium f_{eq} : the first argument of q and q^l in (1.7) and (1.10) is replaced by f_{eq} . Since these terms are of the order of Δt , this modification preserves the consistency of our schemes. Moreover, this allows to obtain self-adjoint operators for the weight $1/f_{eq}$, which is always positive. This property is known for the operator $q(f_{eq}, \cdot)$ which is nothing but the linearized Landau operator at equilibrium f_{eq} . For the operator $q^l(f_{eq}, \cdot)$, this property has already been given in a general frame in proposition 1.1. Moreover, the conservation properties are naturally preserved. Our schemes are the followings.

equilibrium θ -scheme:

$$\frac{f^{n+1} - f^n}{\Delta t} = Q(f^n) + \theta q(f_{eq}, f^{n+1} - f^n). \quad (1.14)$$

equilibrium log-linear scheme:

$$\frac{f^{n+1} - f^n}{\Delta t} = Q(f^n) + q^l(f_{eq}, f^{n+1} - f^n). \quad (1.15)$$

Now, we briefly explain how we solve the linear systems included in the schemes presented above.

1.2 Linear solvers

In this section, we assume that the velocity variable has been discretized (with N points), so that the discrete collision operator also satisfies the conservation and entropy properties. The previous schemes can then be applied without any modification to this discrete version of the FPL equation, and they have the same properties as their continuous versions. Then schemes (1.5), (1.7), (1.10), (1.14), and (1.15) can be seen as linear systems in which the unknown is the vector f^{n+1} . By using simple calculations, all these schemes can be written under the following incremental form

$$(I - \Delta t L) \delta f^n = \Delta t Q(f^n), \quad (1.16)$$

where $\delta f^n = f^{n+1} - f^n$ and L is the linear operator used in the scheme ($L = q^c(f^n, \cdot)$, $\theta q(f^n, \cdot)$, $q^l(f^n, \cdot)$, $q(f_{eq}, \cdot)$ or $q^l(f_{eq}, \cdot)$).

The numerical solving of such a system presents two difficulties. First, this is classical, the algorithm must be fast enough. In particular, since L is usually a dense matrix, using a direct solver like Gauss method is excluded. It is therefore reasonable to use an iterative solver, in which we can also make use of the existing fast algorithms to evaluate the collision operator: such algorithms reduce the cost of a matrix-vector product as if L was a sparse matrix. The other difficulty is due to the conservation properties: even if the solution of the linear system cannot be computed exactly, is it possible to preserve the conservation properties exactly? We have then proved in [2] that all the Krylov solvers (like the Conjugate Gradient) satisfy this property. It relies on very simple arguments that are given below.

First, note that the conservation properties can be simply written by using the following matrix formalism: let M be the matrix which, for every vector $f \in \mathbb{R}^N$ (supposed to approximate a distribution function), associates its moments $Mf \in \mathbb{R}^{d+2}$. For instance, one can set $Mf = \sum_{i=1}^N (1, v_i, \frac{1}{2}|v_i|^2)^T f_i \Delta v^d$ for a regular Cartesian velocity grid. Then, in this discrete frame, the conservation properties of Q and of the linear operators defined above read

$$MQ(f) = 0 \quad \text{and} \quad ML = 0, \quad \forall f \in \mathbb{R}^N.$$

Consequently, the linear system (1.16) reads as the general form

$$Ax = b, \tag{1.17}$$

where the matrix A satisfies the property $MA = M$ and the right-hand-side b satisfies $Mb = 0$ (this allows to obtain $Mx = 0$, that is to say that the moments of f^{n+1} are those of f^n).

Now, we consider an iterative Krylov solver for system (1.17): it can always be put under the following form (see [Saa03])

Algorithm 1.1. 1. give $x^{(0)}$ such that $Mx^{(0)} = 0$ and set $r^{(0)} = b - Ax^{(0)}$;

2. for $k = 1$ to K , find $x^{(k)}$ in the affine subspace $x^{(0)} + \mathcal{K}_k$, where

$$\mathcal{K}_k = \{r^{(0)}, Ar^{(0)}, \dots, A^{k-1}r^{(0)}\}.$$

The idea then is: if the initial data is well chosen, that is to say such that $Mx^{(0)} = 0$ (generally, one takes $x^{(0)} = 0$, which means that the solver is initialized with f^n), then the affine subspace inherits this property, and therefore, every iterate $x^{(k)}$ satisfies $Mx^{(k)} = 0$. More precisely, we have the following proposition.

Proposition 1.2. *All iterative methods that can be set under the form of algorithm 1.1 are conservative. This means that we have $Mx^{(k)} = 0$ for every k .*

Proof. Using the conservation properties on $x^{(0)}$, b , and A , yields

$$Mr^{(0)} = M(b - Ax^{(0)}) = 0 - Mx^{(0)} = 0,$$

and therefore $MA^p r^{(0)} = MAA^{p-1}r^{(0)} = MA^{p-1}r^{(0)} = \dots = Mr^{(0)} = 0$ for every $p \geq 1$. Consequently, we have $M\mathcal{K}_k = \{0\}$, and necessarily $x^{(k)} \in x^{(0)} + \mathcal{K}_k$ implies $Mx^{(k)} = 0$. \square

However, we mention that it seems much more difficult to obtain a similar property for the entropy dissipation. For the moment, this question remains open.

1.3 Application to the isotropic Landau equation

The method presented in the previous sections can be efficiently used as soon as one has a discretization of the velocity variable for which the discrete collision operator is conservative and entropic, and can be rapidly computed. In this section, we restrict ourselves to the case of the isotropic Landau equation. In this model, f depends only on the kinetic energy $\varepsilon = |v|^2$. In [2] and [3], we have used a finite-difference discretization proposed by Berezin, Khudic and Pekker [BKP87] (and also used by Buet and Cordier [BC02]), as well as a multi-wavelet approximation proposed by Antoine and Lemou [AL03]. For these two approximations, the complexity of one evaluation of $Q(f)$ is in $O(N)$, where N is the number of discretization energy points.

Here, we give two significative results in the case of the Coulombian potential. In figure 1.1, we compare the evolution of the entropy obtained with a backward Euler explicit scheme to that obtained with the contracted scheme (1.5). The time step used for the implicit scheme is 50 times as large as that of the explicit scheme, and we observe that the dynamics is correctly described by the implicit scheme. In figure 1.2, we plot the CPU time used by these two schemes as a function of the number of discretization points N . According to our analysis, the CPU time of the explicit scheme is $O(N^3)$, while that of the implicit scheme is $O(N^2)$.

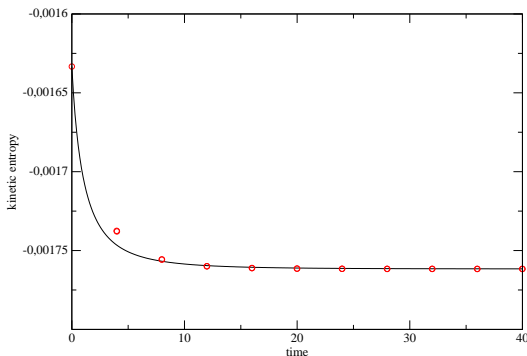


FIG. 1.1: Evolution of the entropy for two explicit (-) and implicit (o) schemes.

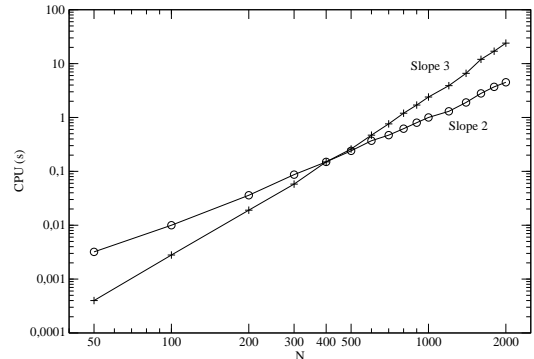


FIG. 1.2: CPU time for two explicit (-) and implicit (o) schemes, as a function of N .

1.4 Perspectives

To apply the previous methods to the three-dimensional Landau equation, we are currently working in the following three directions.

Preconditioning.

It is fundamental to include an efficient preconditioner in our linear solvers. Actually, in three dimensions (3D) with N discretization points, the cost of one simulation for a given physical time is of the order of KN for an implicit scheme, where K is the number of iterations of the linear solver, while it is of the order of $N^{5/3}$ for an explicit scheme. Then K must be much

lower than N to obtain an efficient scheme. If one does not use any preconditioner, K can be of the order of N , which makes the corresponding implicit scheme slower than a simple explicit scheme. However, an efficient preconditioner can render K virtually independent of N . The difficulty in the design of such a preconditioner is that, in addition to the usual constraints, it also must satisfy the conservation properties in order to preserve these of the linear solver. Our idea is then to construct ad hoc preconditioners based on the Landau operator itself, rather than using standard algebraic preconditioners (like incomplete LU) that have no reason to preserve the conservation properties. In the isotropic case, we have tested a preconditioner given by the Landau operator with a Maxwellian potential. It has all the required properties, since it is known that the Maxwellian potential makes the operator linear and local, hence easily invertible, and conservative. Then, it allows to strongly decrease the number of iterations of the linear solver. However, this operator is not self-adjoint; consequently, it cannot be used in the Conjugate Gradient.

Velocity discretization.

The problem of the velocity discretization of the Landau operator is much more difficult in 3D than in 1D. In particular, for a finite difference approximation, it seems that only a discretization on the “Log” form gives stable schemes (see [BC99]). This allows to use the log-linear scheme (or its equilibrium version), but not the contracted or θ -schemes. In addition, the approximation of the 3D Landau operator must be computable with fast algorithms. At present, we use the multipole method adapted to the FPL equation by Lemou [Lem98]: with this method, the complexity of one evaluation of $Q(f)$ is $O(N \log N)$ instead of $O(N^2)$ for a direct evaluation. It would be interesting to test the spectral method of Pareschi, Russo and Toscani [PRT00], and we also think to a possible extension of the multi-wavelet method of Antoine et Lemou [AL03].

Non-linear implicit schemes.

Finally, we mention the fact that the only linear implicit scheme that we have tested in 3D for the moment (the log-linear scheme) does not seem to be very efficient: it looks as if it is stable only for small time steps, which makes it not very competitive. At present, by using the ideas presented in this work, we study a completely non-linear scheme based on the “Log” form, which includes a Newton method whose Jacobian matrix is self-adjoint, and hence invertible by the Conjugate Gradient. This scheme seems more robust than the previous ones.

Chapter 2

Coupling kinetic and fluid models

The simulation of particle systems is a typical example of multiscale problems. Indeed an accurate description of such systems is given by the kinetic theory. But when the system is close to an equilibrium state, it is much simpler and often accurate enough to use macroscopic models like fluid mechanics or diffusion theory. A rough indicator of the validity of a macroscopic approximation is often called the Knudsen number, which can be defined as the ratio of the mean free path of the particles to a typical macroscopic length.

Until a recent period, macroscopic approximations (that we call "fluid" in this article) were used even for systems far from equilibrium, since microscopic theories were too computationally expensive. Nowadays, modern super-computers are able to treat many problems at the kinetic level, but there are still very challenging problems, like that involving different scales. For instance, we mention the simulation of re-entry problems in aerodynamics, where the particles are close to equilibrium far from the re-entry body, while non-equilibrium effects are very large close to the body. For radiative transfer problems, this can occur when the material is composed of several parts of very different opacities. The difficulty is that the computational effort is generally increasing with the inverse of the Knudsen number. Then a large part of the computational time is due to a part of the system (close to equilibrium) that could be more efficiently described by a simpler macroscopic model.

Consequently, it seems very natural to try to solve each model wherever it is appropriate, the main problem being to correctly match the two description at the interfaces of the different domains. This is especially attractive when the particles are in an equilibrium state in the major part of the domain. This idea has been largely explored in the past few years. For problems involving diffusive fluid models (like for neutron and radiative transfer problems) we mention for instance the works of Bal and Maday [BM02], Degond and Schmeiser [DS99], Golse, Jin and Levermore [GJL03], Klar [Kla98a], and Klar and Siedow [KS98]. For rarefied gas dynamics, we mention the works of Bourgat, Le Tallec and Tidriri [BTT96], of Bourgat, Le Tallec, Malinger, and Qiu [Qiu93, TM97], Neunzert, Struckmeier, Klar [KNS00], Schneider [Sch96]. The main common feature of these approaches is that they are typical domain decomposition techniques where the fluid and kinetic models are solved in different subdomains. The coupling relations are defined through suitable boundary conditions at the interface between the subdomains.

Very recently, a different approach has been proposed by Degond and Jin [DJ05] for matching kinetic and diffusion problems. In this work the idea was still to use a domain

decomposition method but in which the coupling is through the equations rather than the boundary conditions.

In this chapter, we present several works that are based on this approach. In section 2.1, we describe an extension of the method of [DJ05] to nonlinear problems, for a hydrodynamic scaling (also called “hyperbolic” scaling). We show a property of homogeneity that must be satisfied by equilibrium distributions to obtain an accurate method. In section 2.2, this approach is extended to a dynamic coupling (i.e. in which the kinetic and fluid domains can change as the time evolves). In section 2.3, this method is deeply modified by using a decomposition of the distribution function into macroscopic and microscopic parts (the so called “micro-macro” decomposition): this allows to obtain a more flexible approach which is closer to multiscale-like approaches than to domain decomposition methods.

2.1 Kinetic/fluid coupling by domain decomposition without interface boundary condition [4]

Here we present a joint work with P. Degond and S. Jin, published in the *Journal of Computational Physics* in 2005 [4].

Let $f(t, x, v)$ be the density of particles that, at time t , have position $x \in \Omega$ and velocity $v \in \mathbb{R}^N$ or any bounded or discrete subset of \mathbb{R}^N . The evolution equation of f is

$$\partial_t f + v \cdot \nabla_x f = \frac{1}{\varepsilon} Q(f), \quad (2.1)$$

with initial data $f(0, x, v) = f_0(x, v)$. The left-hand side of (2.1) describes the motion of the particles of velocity v , while the operator Q takes into account the collisions between particles. The parameter ε is the ratio of the microscopic to the macroscopic scales.

In the sequel, we denote the integral of every vectorial or scalar function $f = f(v)$ by $\langle f \rangle = \int f(v) dv$. The collision operator Q is supposed to satisfy the conservation property

$$\langle mQ(f) \rangle = 0 \quad \text{for every } f,$$

where $m(v) = (m_i(v))_{i=1}^d$ are the locally conserved quantities. Consequently, multiplying (2.1) by m and integrating w.r.t v , we find the local conservation laws

$$\partial_t \langle mf \rangle + \nabla_x \cdot \langle vmf \rangle = 0.$$

Finally, we assume that the local equilibria of Q (i.e., the solutions of $Q(f) = 0$) are the equilibrium distributions $E[\rho]$, implicitly defined by their moments through the relation $\rho = \langle mE[\rho] \rangle$. We do not specify boundary conditions for the moment. When ε tends to 0, (2.1) implies that f converges, formally, towards $E[\rho]$, where $\rho(t, x)$ is a solution to the system

$$\partial_t \rho + \nabla_x \cdot F(\rho) = 0, \quad (2.2)$$

with initial data $\rho|_{t=0} = \langle mf_0(x, v) \rangle$. The flux $F(\rho)$ is the equilibrium kinetic flux

$$F(\rho) = \langle vmE[\rho] \rangle. \quad (2.3)$$

This asymptotic model is often called a “fluid” or macroscopic model, by analogy with the kinetic theory of rarefied gases, in which this asymptotics is nothing but the system of Euler equations of fluid mechanics.

Generally speaking, in the coupling strategy by domain decomposition, it is assumed that the domain Ω can be decomposed into two subdomains: one subdomain contains near equilibrium particles, while the other one contains particles that are far from the equilibrium state. This assumption allows to describe the system by a fluid model like (2.2) in the first subdomain, while the kinetic model (2.1) is more adapted to describe the other subdomain. Generally, this strategy requires, for each model, to define specific boundary conditions at the interface between the subdomains.

Now, we briefly describe below the idea of Degond and Jin [DJ05], rewritten in the hydrodynamic scaling framework, that has been proposed to avoid interface boundary conditions. We introduce un “buffer” zone Ω_B around the interface, so that the domain Ω is now decomposed into three (non overlapped) parts: $\Omega = \Omega_F \cup \Omega_B \cup \Omega_K$. The “fluid” domain (i.e. where the fluid approximation is correct) is denoted by Ω_F and the kinetic domain is denoted by Ω_K (see figure 2.1). Then we introduce a transition function h defined by

$$\begin{cases} h(x) = 1, & \text{for } x \in \Omega_K, \\ h(x) = 0, & \text{for } x \in \Omega_F, \\ 0 \leq h(x) \leq 1 & \text{for } x \in \Omega_B. \end{cases} \quad (2.4)$$

With this function, f is decomposed into a “kinetic” part $f_K = hf$ and a “fluid” part $f_F = (1-h)f$. Note that f_K and f_F satisfy the following properties: they are defined in the whole Ω , we have $f = f_K + f_F$, and finally, by construction of h , these quantities are equal to f in their respective domains Ω_K and Ω_F (see figure 2.2).

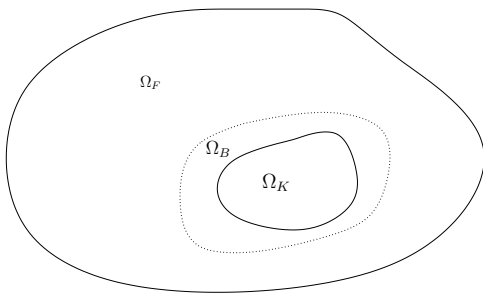


FIG. 2.1: Decomposition of the computational domain Ω into three non-overlapping zones: fluid (Ω_F), kinetic (Ω_K), and buffer (Ω_B).

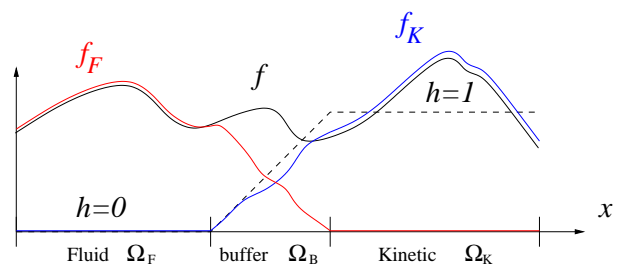


FIG. 2.2: The distribution function f , the transition function h , and the kinetic and fluid parts f_K and f_F (1D view).

It is then easy to obtain the following evolution equations for f_K and f_F :

$$\partial_t f_K + hv \cdot \nabla_x f_K + hv \cdot \nabla_x f_F = \frac{1}{\varepsilon} h Q(f_K + f_F), \quad (2.5)$$

$$\partial_t f_F + (1-h)v \cdot \nabla_x f_F + (1-h)v \cdot \nabla_x f_K = \frac{1}{\varepsilon} (1-h) Q(f_K + f_F), \quad (2.6)$$

with initial data $f_K|_{t=0} = hf_0$ and $f_F|_{t=0} = (1-h)f_0$. This system is formally equivalent to the original equation (2.1).

Then we use the assumption of equilibrium in Ω_F and Ω_B to describe the fluid part with macroscopic parameters. This assumption means $f_F = E[\rho_F]$ in Ω_F and Ω_B , which allows, by taking the moments of (2.6), to transform (2.5)–(2.6) into the coupled system

$$\partial_t f_K + hv \cdot \nabla_x f_K + hv \nabla_x \cdot E[\rho_F] = \frac{1}{\varepsilon} h Q(f_K + E[\rho_F]), \quad (2.7)$$

$$\partial_t \rho_F + (1-h) \nabla_x \cdot F(\rho_F) + (1-h) \nabla_x \cdot \langle mv f_K \rangle = 0, \quad (2.8)$$

with initial conditions $f_K|_{t=0} = hf_0$ and $\rho_F|_{t=0} = (1-h)\rho_0 = \langle m f_0 \rangle$. This model appears as a kinetic equation and a fluid equation, coupled by convection and collision terms. Due to the fluid approximation, this model is no longer equivalent to the original kinetic equation: it simply gives an approximation of f by $f_K + E[\rho_F]$. The justification, even formal, of the passing from (2.5)–(2.6) to (2.7)–(2.8) is not very clear. It would probably require that ε depends on x so as to be small in Ω_F and of order 1 in Ω_K (see [6] for such an analysis for a slightly different model).

Now, we explain the properties of this model. First, an important property is that the kinetic part f_K remains zero in the fluid domain Ω_F , while the fluid part ρ_F remains zero in the kinetic domain Ω_K . Actually, from the definition of h , (2.7) implies $\partial_t f_K = 0$ in Ω_F , and (2.8) implies $\partial_t \rho_F = 0$ in Ω_K . The initial data of (2.7) and (2.8) then imply the announced result. Therefore, in the kinetic domain Ω_K , model (2.7)–(2.8) degenerates into the equation

$$\partial_t f_K + v \cdot \nabla_x f_K = \frac{1}{\varepsilon} Q(f_K), \quad (2.9)$$

which is nothing but the original kinetic equation (2.1). In the fluid domain Ω_F , the model degenerates into

$$\partial_t \rho_F + \nabla_x \cdot F(\rho_F) = 0, \quad (2.10)$$

which is nothing but the fluid approximation (2.2). This is only in the buffer zone Ω_B that the coupling (2.7)–(2.8) is really effective. This shows that this model indeed allows a transition of the kinetic model towards the fluid model, from one domain to the other one, without any interface boundary conditions.

The advantage of this approach, as compared to the classical coupling by interface boundary conditions, is mainly the following. When the interface is complicated, the method of [Qiu93, TM97] needs the implementation of the interface flux condition in a complicated way, while our method based on the introduction of a smoothing function h transfers the geometry to the PDE. This is an advantage, since it is then possible to solve the PDE in a regular geometry while completely ignoring the real interface geometry. One just has to choose h first according to the interface geometry initially, then forget about the geometry and solves the PDE on regular grids. This geometry is taken into account only for the construction of h . Then, in practice, in the computational code, it is sufficient to test the value of f to know if one solves (2.9), (2.10), or (2.7)–(2.8). This approach also allows to make the kinetic and fluid domains change as the time evolves, as it will be shown in section 2.2.

Finally, a last important property is that this model is also able to correctly describe the system if it is in an equilibrium state in the whole Ω : actually, if ε tends to 0 in (2.7)–(2.8), we easily prove that the sum of the moments $\langle mf_K \rangle + \rho_F$ satisfy at the limit the fluid equation (2.2).

However, we have remarked in [4] that this approach as an important drawback: the uniform states are preserved only for some specific kinetic models. For other models, oscillations can be generated. Namely, we have the following proposition:

Proposition 2.1. *Assume the mapping $\rho \mapsto E[\rho]$ is homogeneous of degree 1, that is*

$$E[\lambda\rho] = \lambda E[\rho] \quad (2.11)$$

for every $\lambda \geq 0$ and every ρ in the definition domain of E . If the initial condition f^0 is a constant equilibrium $E[\rho]$, then $f_K = hE[\rho]$ and $\rho_F = (1 - h)\rho$ are solutions of the coupled model (2.7)–(2.8), and $f_K + E[\rho_F] = E[\rho]$.

This property is satisfied by the collision operators based on the Maxwell-Boltzmann statistics. But this is not true for the Fermi-Dirac statistics, or even simply for the following toy model

$$\partial_t u + \partial_x u = \frac{1}{\varepsilon}(M_1[\rho] - u), \quad \partial_t v - \partial_x v = \frac{1}{\varepsilon}(M_2[\rho] - v), \quad (2.12)$$

where the equilibrium is $(M_1[\rho], M_2[\rho]) = \frac{1}{2}(\rho + f(\rho), \rho - f(\rho))$, with $f(\rho) = \frac{1}{2}\rho^2$ and $\rho = u + v$. This model has the same form as (2.1) with discrete velocities $v = \pm 1$ and the collisional invariant $m(v) = 1$. It can be proved that it converges to the Burgers equation $\partial_t \rho + \partial_x f(\rho) = 0$ when $\varepsilon \rightarrow 0$. It is clear that the equilibrium is not a homogeneous function of ρ . In that case, simple calculations show that the conclusions of proposition 2.1 are false. As a consequence, the coupled model derived from this system cannot correctly describe the solution where it is constant. This will be shown at the end of this section.

From the numerical point of view, we have proposed a simple discretization of (2.7)–(2.8), obtained in the following way. First, we discretize the kinetic equation (2.1) with a standard finite-volume scheme, explicit in time, with upwinding. Then we apply to this scheme the same derivation as explained above in the continuous case (splitting of f into f_K and f_F , then using the fluid approximation in $\Omega_F \cup \Omega_B$). To simplify, we write below the scheme we obtain in one space dimension:

$$\begin{aligned} \frac{f_{K,i}^{n+1} - f_{K,i}^n}{\Delta t} + h_i \frac{\phi_{i+\frac{1}{2}}(f_K^n) - \phi_{i-\frac{1}{2}}(f_K^n)}{\Delta x} + h_i \frac{\phi_{i+\frac{1}{2}}(E[\rho_F^n]) - \phi_{i-\frac{1}{2}}(E[\rho_F^n])}{\Delta x} \\ = h_i Q(f_{K,i}^n + E[\rho_{F,i}^n]), \end{aligned} \quad (2.13)$$

$$\frac{\rho_{F,i}^{n+1} - \rho_{F,i}^n}{\Delta t} + (1 - h_i) \frac{F_{i+\frac{1}{2}}(\rho_F^n) - F_{i-\frac{1}{2}}(\rho_F^n)}{\Delta x} + (1 - h_i) \frac{\left\langle m \left(\phi_{i+\frac{1}{2}}(f_K^n) - \phi_{i-\frac{1}{2}}(f_K^n) \right) \right\rangle}{\Delta x} = 0, \quad (2.14)$$

where the numerical flux is defined by $\phi_{i+\frac{1}{2}}(g) = v^- g_{i+1} + v^+ g_i$, and the numerical equilibrium flux is $F_{i+\frac{1}{2}}(\rho_F) = \langle m \phi_{i+\frac{1}{2}}(E[\rho_F]) \rangle$, which is a consistent approximation of $F(\rho_F)$ (of kind "kinetic flux splitting", see [MD94]).

Finally, we mention a remarkable property of our method: when the buffer zone reduces to an interface, we could have proved simply that our scheme can be written as a coupling method by half-fluxes like that of [Qiu93, TM97] (see [4]).

Before we conclude this section, we show two comparisons between a fully kinetic simulation and a result obtained with our coupling method. In figure 2.3, we plot the results obtained with two different initial data: one is constant (left), and the other one is discontinuous (right). In both cases, the test is carried out for the toy model (2.12): one can clearly see, in the buffer zone, the jump artificially generated by the non preservation of uniform flows. In figure 2.4, we plot the results obtained with the BGK model of the rarefied gas dynamics, on a two-dimensional test. We observe the diffraction of a plane shock wave on a cylinder: the results of the full kinetic model and of the coupled model are very close. Note that the boundaries of the kinetic and fluid domains are not aligned on the mesh (which is curvilinear): the flexibility of our method allows to treat this complex geometry in a transparent way.

As a conclusion, however, we mention two important drawbacks of our method. It must be noted that the preservation of uniform flows requires, at the numerical level, that the macroscopic fluxes $F(\rho_F)$ and $\langle mvf_K \rangle$ in (2.8) are discretized with the same method. This is indeed satisfied with the discretization detailed above, but this cannot be true if $F(\rho_F)$ is discretized with a standard scheme of the Computational Fluid Dynamics (Roe, Osher, etc.). One can try to neglect these effects due to the non-preservation of uniform flows (they are of the order of the discretization step), but one then has to face another problem, namely an artificial “cavitation” problem: by construction, the density associated to ρ_F becomes very small for x close to Ω_K . It is therefore necessary to use a scheme which is robust for such a phenomenon (like the kinetic discretization presented above, but not like the Roe scheme, for instance). The method presented in [6] (see section 2.3) gives a solution to these two problems.

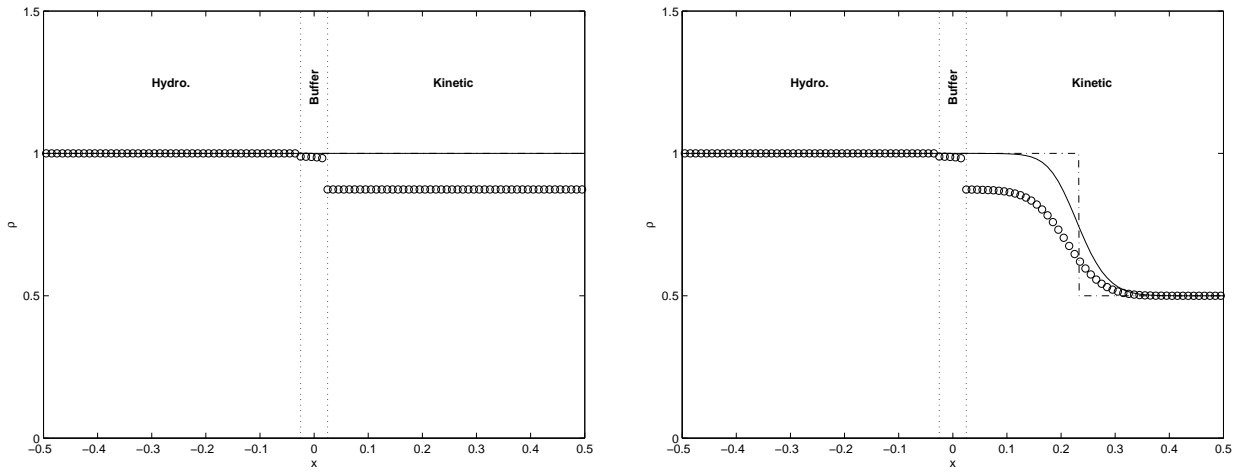


FIG. 2.3: Comparison between the kinetic model (2.12) and the coupled model (2.7)–(2.8). Stationary result for a constant initial data (left), result at $t = 0.3150$ for a discontinuous initial data (right). Legend: kinetic (-), coupling (o), fluid (-.).

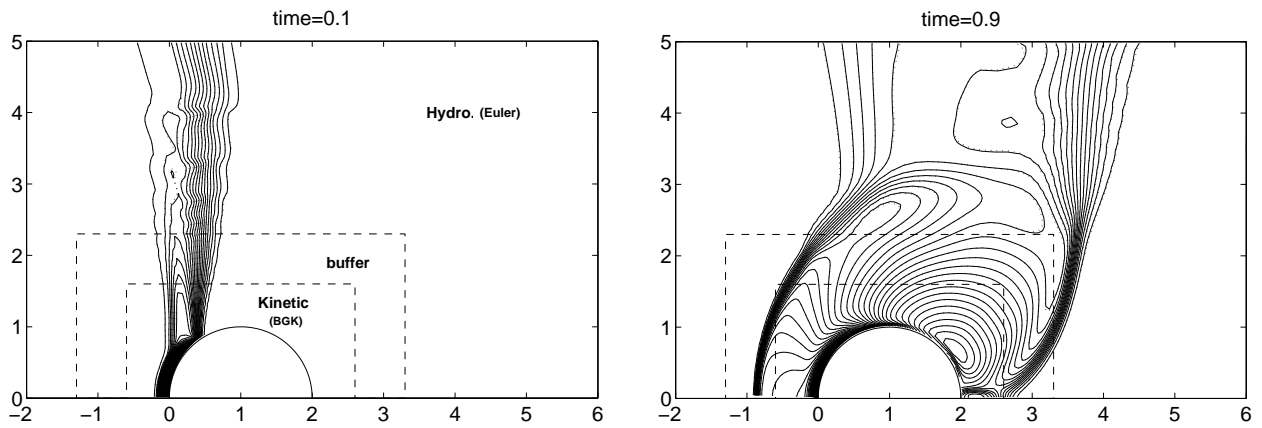


FIG. 2.4: Diffraction of a shock on a cylinder in a rarefied gas, with $\text{Knudsen}=0.005$ and $\text{Mach}=2.81$. Density contours at $t = 0.1$ and $t = 0.9$ for the coupled model (continuous lines) and the BGK model (dotted lines).

2.2 Kinetic/fluid coupling with a moving interface [5]

We summarize below, very briefly, the joint work with P. Degond and G. Dimarco, to appear in the Journal of Computational Physics [5].

We have already shown in [4] that it is possible to make domains Ω_K and Ω_F evolve by using a transition function h that also depends on time. Following the same approach as in section 2.1, we get the following coupled model

$$\partial_t f_K + hv \cdot \nabla_x f_K + hv \nabla_x \cdot E[\rho_F] = \frac{1}{\varepsilon} h Q(f_K + E[\rho_F]) - (f_K + E[\rho_F]) \partial_t h, \quad (2.15)$$

$$\partial_t \rho_F + (1-h) \nabla_x \cdot F(\rho_F) + (1-h) \nabla_x \cdot \langle mv f_K \rangle = (\rho_F + \langle m f_K \rangle) \partial_t h, \quad (2.16)$$

where the only differences, in comparison to system (2.7)–(2.8), are the new terms $\partial_t h$ in the right-hand sides. This model can be discretized in the same way as the model with a steady h (see (2.13)–(2.14)), but with the following approximation for the new terms: $(f_{K,i}^n + E[\rho_{F,i}^n]) \frac{h_i^{n+1} - h_i^n}{\Delta t}$ and $(\rho_{F,i}^n + \langle m f_{K,i}^n \rangle) \frac{h_i^{n+1} - h_i^n}{\Delta t}$.

The main difficulty is to define how the transition function h can evolve. There exist a few cases in neutron transport or in radiative transfer where the evolution of the interface is known a priori. But in other cases, like in aerodynamics, this evolution is not known. In [5], we addressed this problem for the (Boltzmann-BGK)/Euler coupling. We proposed an evolution of h following two criteria :

- a microscopic criterion, based on the work by Dimarco and Pareschi [DP], which gives some measure β of the distance between the distribution function and its local equilibrium: for a distribution function f and its Maxwellian $M[f]$, we compute the largest value β such that $\beta M[f]$ is lower than f for every v . Due to its cost, this criteria is used only in Ω_K ;
- a macroscopic criterion of kind “local Knudsen number” that compares a macroscopic distance, based on a “gradient length” and a microscopic distance like the mean free path.

A combination of these two criteria allows to compute a new h at each time step.

We conclude this section by two numerical results taken from [5]. In figure 2.5, we show the evolution of a 1D shock, reflected by a wall located at $x = 0$. At $t = 0$, the computational domain is divided into one kinetic zone and one fluid zone. After the reflection, when the shock is sufficiently far from the wall, the gas is sufficiently close to the equilibrium upstream from the shock: then, the algorithm automatically creates a second fluid zone. One can then see the different zones moving as the time evolves. In figure 2.6 is shown the classical Sod test, computed with two fluid zones and one kinetic zone. We observe that the kinetic zone follows the shock and the contact discontinuity, but not the rarefaction wave, that is described by the fluid model. In both tests, we do not observe any difference between the full kinetic simulation and our coupling, whereas the full fluid model shows some differences in the kinetic zones.

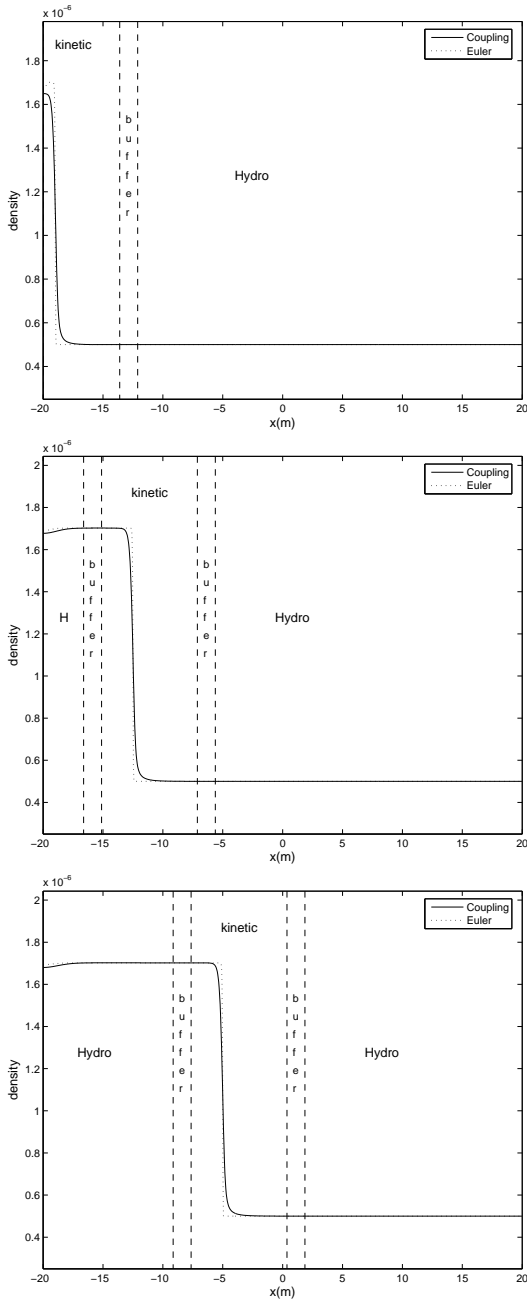


FIG. 2.5: Reflected shock: density at $t = 0.002$ (top), $t = 0.02$ (middle), $t = 0.04$ (bottom). Comparison coupling (-) and Euler (.).

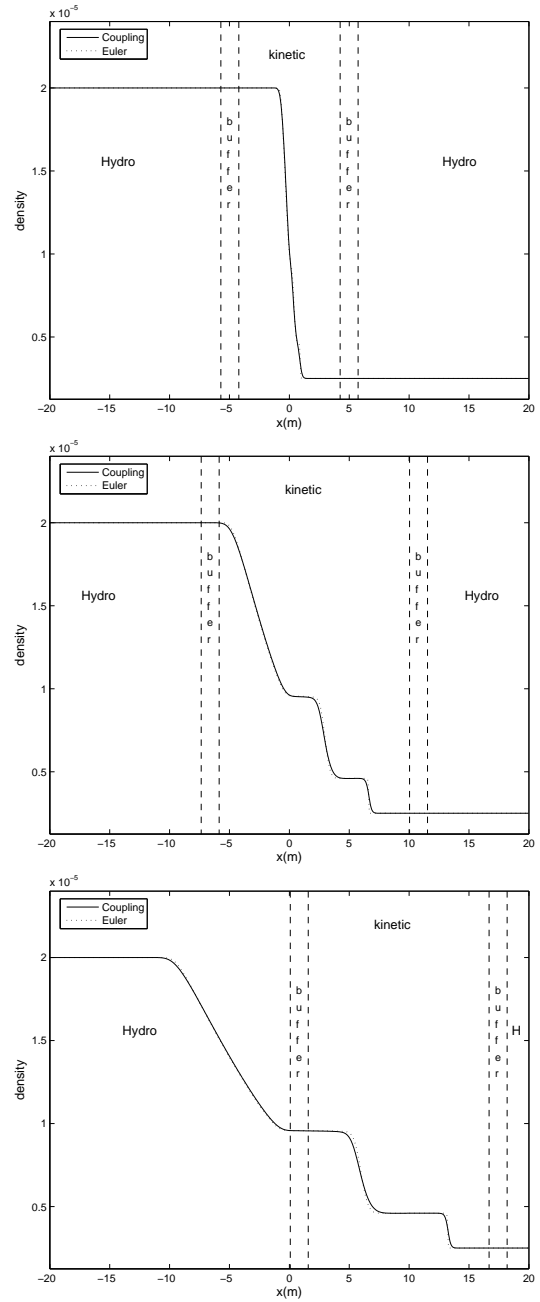


FIG. 2.6: Sod test: density at $t = 0.002$ (top), $t = 0.015$ (middle), $t = 0.03$ (bottom). Comparison coupling (-) and Euler (.).

2.3 Fluid model with local kinetic upscalings [6]

Here, we summarize the joint work with P. Degond and J.-G. Liu, and published in *SIAM Multiscale Modeling & Simulation* in 2006 [6].

Although this new method was first designed as a slight modification of the method presented in section 2.1 (so as to avoid the drawback of non-preservation of uniform flows), it finally appears as a very different approach. The model we obtain can actually be seen as a fluid model, used in the whole domain Ω , which is *locally* corrected by a kinetic upscaling in non-equilibrium zones. This upscaling is obtained by solving a kinetic equation for the non-equilibrium part of the distribution function. This equation is solved only locally and is related to the fluid equation through a downscaling effect. This approach is mainly based on two ideas:

- the micro-macro decomposition is used to separate f in the whole domain into an equilibrium part (called fluid, or macroscopic), and a non-equilibrium part (kinetic, or microscopic);
- the transition function h , introduced section 2.1, is used to localize the non-equilibrium part.

We briefly detail below how we apply these two ideas. Since this method can be applied to hydrodynamic and diffusion scalings, we first consider a general kinetic equation, written in a dimensional form:

$$\partial_t f + v \cdot \nabla_x f = Q(f), \quad (2.17)$$

with the initial data $f(0, x, v) = f_0(x, v)$. The collision operator satisfies the classical properties given in section 2.1. The micro-macro decomposition of f is

$$f = E[\rho] + g, \quad (2.18)$$

where $E[\rho]$ is the local equilibrium associated to the moments $\rho = \langle mf \rangle$, and g is the difference between f and $E[\rho]$. We easily get the following proposition:

Proposition 2.2. *If $\rho = \langle mf \rangle$ and $g = f - E[\rho]$, then they satisfy the following coupled equations:*

$$\partial_t \rho + \nabla_x \cdot F(\rho) + \nabla_x \cdot \langle vmg \rangle = 0, \quad (2.19)$$

$$\partial_t g + v \cdot \nabla_x g = Q(E[\rho] + g) - (\partial_t + v \cdot \nabla_x)E[\rho], \quad (2.20)$$

where $F(\rho) = \langle vmE[\rho] \rangle$ is the equilibrium flux vector. The associated initial data are

$$\rho|_{t=0} = \rho_0 = \langle mf_0 \rangle \quad \text{and} \quad g|_{t=0} = f_0 - E[\rho_0].$$

Reciprocally, if ρ and g satisfy this system, then $f = E[\rho] + g$ satisfies the kinetic equation (2.17), and we have $\rho = \langle mf \rangle$ and $\langle mg \rangle = 0$.

Then equation (2.19) can be seen as a fluid model with a “kinetic upscaling” $\nabla_x \cdot \langle vmg \rangle$. Note that this model can be made more elegant if the time derivative $\partial_t E[\rho]$ is eliminated in (2.20). This has been done in [7], after the present work, for the construction of asymptotic preserving schemes (see section 3.1).

Next, we use the transition function h defined by (2.4) (section 2.1), as well as the domains Ω_F , Ω_B , and Ω_K . This function is used to localize the non-equilibrium part g : the method described section 2.1 is then applied to separate g into $g = g_K + g_F$, with $g_K = hg$ and $g_F = (1 - h)g$, and we obtain the following model

$$\partial_t \rho + \nabla_x \cdot F(\rho) + \nabla_x \cdot \langle vmg_K \rangle + \nabla_x \cdot \langle vmg_F \rangle = 0, \quad (2.21)$$

$$\partial_t g_K + hv \cdot \nabla_x g_K + hv \cdot \nabla_x g_F = hQ(E[\rho] + g_K + g_F) - h(\partial_t + v \cdot \nabla_x)E[\rho], \quad (2.22)$$

$$\begin{aligned} \partial_t g_F + (1 - h)v \cdot \nabla_x g_F + (1 - h)v \cdot \nabla_x g_K &= (1 - h)Q(E[\rho] + g_K + g_F) \\ &\quad - (1 - h)(\partial_t + v \cdot \nabla_x)E[\rho]. \end{aligned} \quad (2.23)$$

which is also equivalent to (2.17). The non-equilibrium part is then localized by using the assumption of equilibrium in $\Omega_F \cup \Omega_B$: contrary to the method of section 2.1, this does not mean that g_F is replaced by $E[\rho_F]$ but rather that g_F is small, which is a consequence of the definition of g . Practically, the calculations needed for this localization procedure depend on the scaling (hydrodynamic or diffusion). We give below the results obtained for both scalings.

For the hydrodynamic scaling, we use new time and space variables $x' = \varepsilon x$ and $t' = \varepsilon t$, which is equivalent to replace Q by $\frac{1}{\varepsilon}Q$ in the previous relations. Using the equilibrium assumption in $\Omega_F \cup \Omega_B$, g_F is then eliminated from equations (2.21)–(2.23) (see some arguments in section 3.2 of [6]) to obtain the following model:

$$\partial_t \rho + \nabla_x \cdot F(\rho) + \nabla_x \cdot \langle vmg_K \rangle = 0, \quad (2.24)$$

$$\partial_t g_K + hv \cdot \nabla_x g_K = \frac{h}{\varepsilon}Q(E[\rho] + g_K) - h(\partial_t + v \cdot \nabla_x)E[\rho], \quad (2.25)$$

where the kinetic part g_K plays a role only in $\Omega_K \cup \Omega_B$ that should be seen as a union of small zones in which a kinetic description is necessary. In the other parts of the domain, only the fluid equation (2.24) with $g_K = 0$ is solved. In this interpretation, the notion of domain decomposition almost completely disappears. Since, by construction, the function h is not applied to the fluid part, it is then not surprising that, contrary to the method of section 2.1, this model is uniform flow preserving, whatever the collision operator.

For the diffusion scaling, we considered two examples in [6]: the linear transport and the radiative heat transfer (both in one space dimension only). This scaling requires the new variables $x' = \varepsilon x$ and $t' = \varepsilon^2 t$, which means that ∇_x and ∂_t are replaced by $\varepsilon \nabla_x$ and $\varepsilon^2 \partial_t$ in equations (2.21)–(2.23). For the linear transport, the collision operator is $Q(f) = \sigma(\int_{-1}^1 f dv - f)$ and only the density $\rho = \langle f \rangle$ is conserved. Without going into details, we give

below the kinetic model, the fluid limit (diffusion), the fluid model with kinetic upscaling (system with ρ, g), and the fluid model with localized kinetic upscaling (system with ρ, g_K) :

kinetic model:

$$\varepsilon \partial_t f + v \partial_x f = \frac{1}{\varepsilon} Q(f),$$

fluid limit:

$$\partial_t \rho - \partial_x \left(\frac{1}{3\sigma} \partial_x \rho \right) = 0.$$

fluid model with kinetic upscaling:

$$\begin{aligned} \varepsilon \partial_t \rho + \partial_x \langle v g \rangle &= 0, \\ \varepsilon^2 \partial_t g + \varepsilon v \partial_x g &= -\sigma g - \frac{1}{2} (\varepsilon^2 \partial_t + \varepsilon v \partial_x) \rho, \end{aligned}$$

fluid model with localized kinetic upscaling:

$$\begin{aligned} \partial_t \rho - \partial_x \left(\frac{1}{3\sigma} \partial_x \rho \right) + \partial_x \left(\frac{1}{3\sigma} h \partial_x \rho + \frac{1}{\varepsilon} \langle v g_K \rangle \right) &= 0, \\ \varepsilon^2 \partial_t g_K + \varepsilon h v \partial_x g_K + \varepsilon h v \partial_x g_F &= -\sigma g_K - \frac{1}{2} h (\varepsilon^2 \partial_t + \varepsilon v \partial_x) \rho, \end{aligned}$$

where g_F is

$$g_F = -\varepsilon \frac{1}{2\sigma} (1 - h) v \partial_x \rho.$$

This last model is obtained by using a Hilbert expansion of the kinetic equation associated to $g_F = (1 - h)g$ (see details in [6]). Again, we observe that the model is a fluid equation set in the whole domain Ω : it has the same form as the diffusion equation, but is locally corrected in Ω_K . In comparison with the hydrodynamic scaling, the local correction here contains a macroscopic term.

The radiative heat transfer equation is a more complex model that contains a macroscopic equation for the matter temperature. Our method nevertheless also applies to this case, but we refer to [6] for more details.

At the numerical level, the discretization of our fluid models with kinetic upscalings can be obtained as in the previous method. This is even more flexible here: since the localization does not affect the fluid part, the macroscopic fluxes can be approximated with any method, without generating oscillations or cavitation phenomena.

We conclude this section with two numerical results. In figure 2.7, we plot the results obtained with the same test as in figure 2.3 (page 23). We clearly see that, with this new method, the coupling gives the same result as the kinetic model: the jump at the interface has disappeared, as a consequence of the preservation of uniform flows by the new method. In figure 2.8, we show a comparison between the radiative heat transfer model, our fluid model with localized kinetic upscaling, and the limit diffusion equation. The matter has two very different opacities, and the zones Ω_F , Ω_B , and Ω_K are located accordingly. We observe a perfect agreement between the kinetic solution and our fluid model, while the diffusion limit is completely wrong.

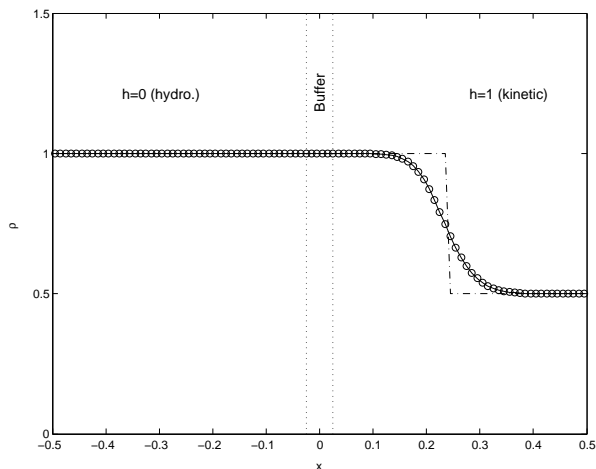


FIG. 2.7: Toy model (2.12) (to be compared with figure 2.3 (page 23)): kinetic solution (-), fluid model with localized kinetic upscaling (o), and fluid limit (-.).

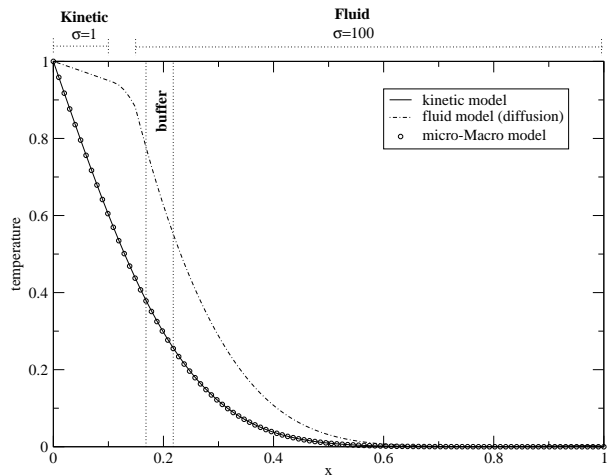


FIG. 2.8: Temperature for the radiative heat transfer at $t = 0.0185$.

2.4 Perspectives

Due to the strong properties of the kinetic upscaling method of section 2.3 (generality, flexibility, robustness), a few extensions of this method will be considered, rather than extensions of the method presented in section 2.1.

Two-dimensional computations

A first project (a joint work in progress with G. Dimarco) is an extension of our method to two space dimension cases (2D). It only requires to adapt the 2D code written for the first method.

Dynamical coupling

It is also important to propose an extension of this approach to the dynamical coupling, by using the ideas proposed in [5]. More intensive researches on the localization criteria should be necessary, as well as deeper investigations at the algorithmic level (in [5], the mesh is too systematically used by the algorithm to define the function h).

Boltzmann/Navier-Stokes coupling

In the case of the hydrodynamic coupling, this method has been applied to the Boltzmann/Euler coupling only. In a work in progress with J.-G. Liu, we try to extend it to a Boltzmann/Navier-Stokes coupling, which is very important for applications.

Using “Asymptotic Preserving” schemes

To obtain a sufficiently accurate method, the buffer zone must be located where the particles are close to the equilibrium. Consequently, the discretization of the kinetic equation must be

efficient both in the kinetic and fluid regimes. This property is typically that of “Asymptotic Preserving” (AP) schemes. Such a scheme has for instance been proposed by Degond and Jin for their coupling method [DJ05]. In a framework similar to that of section 2.3, we have shown, with M. Bennoune and M. Lemou, that the micro-macro decomposition presented in this chapter allows to construct AP schemes (see next chapter). Consequently, using these schemes in our coupling method looks very natural.

Chapter 3

Asymptotic preserving numerical methods for kinetic equations in the fluid limit

In this chapter, we are still interested in the same problem: how to efficiently simulate a particle system when the computational domain contains both non equilibrium zones and fluid zones? While this problem was investigated in chapter 2 by the coupling strategy, we are interested here in constructing numerical approximations of kinetic equations that “mimic” the asymptotic behaviors of the equations. That is to say, these approximations should, somehow, turn into approximations of the asymptotic fluid model when the scaling parameter tends to 0, without any restrictive condition on the numerical parameters of the method. More precisely, we look for numerical schemes that have two essential properties:

- uniform stability in time with respect to ε ;
- the schemes obtained in the fluid regime ($\varepsilon \ll 1$ and $\varepsilon = 0$) must be consistent with the corresponding fluid models.

Such schemes are called “Asymptotic Preserving” (AP) schemes, following the terminology introduced by Jin in [Jin99].

In both works presented here, we have proposed new AP schemes, by using the micro-macro decomposition already mentioned in chapter 2. Note that the preservation of the diffusion limit at the numerical level has been widely investigated, in particular by Klar in [Kla98b, Kla99a, Kla99b], and by Jin (with other collaborators) in [JPT98, Jin99, JPT00, JP01, JP00]. Klar uses a decomposition of the distribution function which is close to the micro-macro decomposition, but he does not fully use the macroscopic nature of the equilibrium part of f . Moreover, he classically uses a time splitting scheme for the collisions. Jin uses a decomposition related to the symmetry of the collision operator (even-odd symmetry). Again, this decomposition is close to the micro-macro decomposition, but it is less general. The stiffness of the collision operator is also treated by the splitting method, and the stiffness due to the transport is removed by the relaxation schemes theory.

Even if the methods presented in those works are quite close to ours, they do not make use of the micro-macro decomposition as systematically as we do. Moreover, we show that it is not necessary to use the classical time splitting to treat the collisions. Finally, our approach is general enough to allow for both hydrodynamic (section 3.1) and diffusion limits (section 3.2).

3.1 Numerical scheme for the Boltzmann equation preserving the compressible Navier-Stokes asymptotics [7]

This work is a part of the thesis of my Ph.D. student M. Bennoune (co-advised with M. Lemou). The corresponding article [7] has been accepted in 2007 for publication in the *Journal of Computational Physics*.

The Boltzmann equation of gas dynamics under non-dimensional form is

$$\partial_t f + v \cdot \nabla_x f = \frac{1}{\varepsilon} Q(f, f), \quad t > 0, (x, v) \in \mathbb{R}^d \times \mathbb{R}^d, \quad (3.1)$$

where the collision operator Q is a bilinear functional and acts only on the velocity dependence of the distribution function f . In all that follows, we use the notations

$$m(v) = \left(1, v, \frac{|v|^2}{2}\right), \quad \text{and} \quad \langle g \rangle = \int_{\mathbb{R}^d} g(v) dv \quad (3.2)$$

for any scalar or vector function $g = g(v)$. The Boltzmann operator $Q(f, f)$ satisfies the conservation properties of the density, momentum, and energy, the entropy inequality, and possesses Maxwellian equilibrium states.

When ε tends to 0, it is known that the moments of f (denoted by $U = (\rho, \rho u, \frac{1}{2}\rho|u|^2 + \frac{d}{2}\rho T) = \langle mf \rangle$) satisfy at the limit the compressible Euler equations

$$\partial_t U + \nabla_x \cdot F(U) = 0, \quad (3.3)$$

where $F(U) = \langle vmM(U) \rangle$ are equilibrium fluxes and $M(U)$ is the local Maxwellian equilibrium corresponding to f . For a finite ε , the Chapman-Enskog method allows to prove that the moments of f are approximated, up to ε^2 , by the solution of the compressible Navier-Stokes equations (CNS)

$$\partial_t U + \nabla_x \cdot F(U) = -\varepsilon \begin{pmatrix} 0 \\ \nabla_x \cdot \sigma \\ \nabla_x \cdot (\sigma u + q) \end{pmatrix}, \quad (3.4)$$

where $\sigma = -\mu \left(\nabla_x u + (\nabla_x u)^T - \frac{2}{d} \nabla_x \cdot u I \right)$ and $q = -\kappa \nabla_x T$ are the shear stress tensor and the heat flux, divided by ε . The diffusive fluxes in the right-hand sides of these equations are of the order of ε and can be viewed as approximations, up to ε^2 , of the difference $\langle vm(f - M(U)) \rangle$ of the fluxes of f and its associated Maxwellian. We refer to the paper by Bardos, Golse, and Levermore [BGL91] for details on this construction.

It is not very difficult to design a numerical scheme for (3.1) that preserves the Euler asymptotics (3.3): it is sufficient to use a splitting between the transport and the collision, then to solve the collision step by a scheme uniformly stable with respect to ε . We refer to the method of Perthame and Coron [CP91] for the case of the BGK operator, and to the more recent work of Gabetta, Pareschi, and Toscani [GPT97] for the Boltzmann operator. However, we have shown in [7] that such a scheme cannot preserve the CNS asymptotics (3.4): more precisely, there is no term of the order of ε in the discrete fluid asymptotics.

Let us rapidly prove this assertion in the case of the BGK equation $\partial_t f + v \cdot \nabla_x f = \frac{1}{\varepsilon}(M(U) - f)$. To simplify, we keep the space variable continuous: the scheme of [CP91] consists in one transport step

$$\frac{f^{n+\frac{1}{2}} - f^n}{\Delta t} + v \cdot \nabla_x f^n = 0,$$

followed by a collision step which is exactly solved

$$f^{n+1} = e^{-\Delta t/\varepsilon} f^{n+\frac{1}{2}} + (1 - e^{-\Delta t/\varepsilon}) M(U^{n+\frac{1}{2}}).$$

Since this step conserves the moments, we have $M(U^{n+\frac{1}{2}}) = M(U^{n+1})$ and we can write f^{n+1} as

$$f^{n+1} = M(U^{n+1}) + e^{-\Delta t/\varepsilon} (f^{n+\frac{1}{2}} - M(U^{n+\frac{1}{2}})).$$

Now, since $e^{-\Delta t/\varepsilon}$ tends to 0 faster than any power of ε , it is therefore impossible to obtain a flux difference $\langle vm(f - M(U)) \rangle$ that is of the order of ε , which gives the result. We have proved in [7] that this drawback can be corrected by replacing the exact solving of the collision phase by a forward Euler implicit scheme: the factor $e^{-\Delta t/\varepsilon}$ is then replaced by $\frac{1}{1+\Delta t/\varepsilon}$ that has the correct asymptotic behavior. However, using the same trick for the Boltzmann operator seems more difficult, and is the subject of an ongoing work.

Then we have proposed a different method, based on the micro-macro decomposition: our idea is to introduce in the Boltzmann equation, without approximation, the decomposition

$$f = M(U) + \varepsilon g, \tag{3.5}$$

where the Maxwellian $M(U)$ associated to f represents the macroscopic part of the system, while g represents the microscopic (or non-equilibrium) part. Next, using the projection operator $\Pi_{M(U)}$ onto the kernel of $\mathcal{L}_{M(U)}$ (which is the linearized Boltzmann operator around $M(U)$), the quantities U and g are separated to obtain the following coupled system, equivalent to the Boltzmann equation (3.1):

$$\partial_t U + \nabla_x \cdot F(U) + \varepsilon \nabla_x \cdot \langle vmg \rangle = 0, \tag{3.6}$$

$$\partial_t g + (I - \Pi_{M(U)})(v \cdot \nabla_x g) = \frac{1}{\varepsilon} \mathcal{L}_{M(U)} g + Q(g, g) - \frac{1}{\varepsilon} (I - \Pi_{M(U)})(v \cdot \nabla_x M(U)). \tag{3.7}$$

This system looks like the one obtained section 2.3. The difference is due to the use of the projection $\Pi_{M(U)}$ which allows to eliminate the time derivative of the Maxwellian. This

decomposition also allows to obtain the CNS equations in a very natural way, since (3.7) directly gives the following expression of the non equilibrium flux of (3.6) :

$$\varepsilon \langle vmg \rangle = \varepsilon \left\langle vm \mathcal{L}_{M(U)}^{-1} (I - \Pi_{M(U)}) (v \cdot \nabla_x M(U)) \right\rangle + O(\varepsilon^2).$$

Classical calculations show that this expression is nothing but the diffusive fluxes of the CNS equations (see for instance [Lev96]). Up to our knowledge, this projection technique has been first presented with this formalism by Degond and Lemou in [DL01], even if similar ideas have already been proposed by Caffisch in [Caf80].

Now, we introduce a time discretization of (3.6)–(3.7) in which the fewest implicit terms are used. The main stiffness is due to the collision term $\frac{1}{\varepsilon} \mathcal{L}_{M(U)} g$ which is taken implicit, while the term $\frac{1}{\varepsilon} (I - \Pi_{M(U)}) (v \cdot \nabla_x M(U))$ is kept explicit. Then, in order to obtain correct diffusion terms in the Chapman-Enskog expansion, the non-equilibrium fluxes $\nabla_x \cdot \langle vmg \rangle$ in the fluid equation (3.6) are taken implicit. Consequently, we obtain the following semi-discrete scheme

$$\frac{U^{n+1} - U^n}{\Delta t} + \nabla_x \cdot F(U^n) + \varepsilon \nabla_x \cdot \langle vmg^{n+1} \rangle = 0, \quad (3.8)$$

$$\begin{aligned} \frac{g^{n+1} - g^n}{\Delta t} + (I - \Pi_{M(U^n)}) (v \cdot \nabla_x g^n) &= \frac{1}{\varepsilon} \mathcal{L}_{M(U^n)} g^{n+1} + Q(g^n, g^n) \\ &\quad - \frac{1}{\varepsilon} (I - \Pi_{M(U^n)}) (v \cdot \nabla_x M(U^n)). \end{aligned} \quad (3.9)$$

As in the continuous case, it is therefore very easy to prove that this scheme gives, up to $O(\varepsilon^2)$, a time explicit scheme which is consistent with the CNS equations.

Finally, in the simplified one-dimensional case, we propose a discretization with staggered grids (which is classical for discretizing second order derivatives). The macroscopic quantities are discretized by $U_i = U(x_i)$ at points $x_i = i\Delta x$, while the microscopic part is discretized by $g_{i+\frac{1}{2}} = g(x_{i+\frac{1}{2}})$ with $x_{i+\frac{1}{2}} = (i + \frac{1}{2})\Delta x$. To obtain a stable scheme in the kinetic regime ($\varepsilon = 1$), we use an upwind discretization of the transport term $(I - \Pi_M)(v \cdot \nabla_x g)$. The other gradients are discretized with central differences, so as to obtain a correct approximation of the diffusion terms in the CNS equations. The scheme we obtain is the following:

$$\frac{U_i^{n+1} - U_i^n}{\Delta t} + \frac{F_{i+\frac{1}{2}}(U^n) - F_{i-\frac{1}{2}}(U^n)}{\Delta x} + \varepsilon \left\langle vm \frac{g_{i+\frac{1}{2}}^{n+1} - g_{i-\frac{1}{2}}^{n+1}}{\Delta x} \right\rangle = 0, \quad (3.10)$$

$$\begin{aligned} \frac{g_{i+\frac{1}{2}}^{n+1} - g_{i+\frac{1}{2}}^n}{\Delta t} + (I - \Pi_{i+\frac{1}{2}}^n) \left(v^+ \frac{g_{i+\frac{1}{2}}^n - g_{i-\frac{1}{2}}^n}{\Delta x} + v^- \frac{g_{i+\frac{3}{2}}^n - g_{i+\frac{1}{2}}^n}{\Delta x} \right) \\ = \frac{1}{\varepsilon} \mathcal{L}_{M_{i+\frac{1}{2}}^n} g_{i+\frac{1}{2}}^{n+1} + Q(g_{i+\frac{1}{2}}^n, g_{i+\frac{1}{2}}^n) - \frac{1}{\varepsilon} (I - \Pi_{i+\frac{1}{2}}^n) \left(v \frac{M_{i+1}^n - M_i^n}{\Delta x} \right), \end{aligned} \quad (3.11)$$

where, to simplify these relations, we denote

$$M_i^n = M(U_i^n), \quad M_{i+\frac{1}{2}}^n = M(U_{i+\frac{1}{2}}^n), \quad \text{and} \quad \Pi_{i+\frac{1}{2}}^n = \Pi_{M_{i+\frac{1}{2}}^n}.$$

The divergence $\nabla_x \cdot F(U)$ can be approximated by any usual scheme, which is not precised here. Then we can prove that this scheme is asymptotically equivalent, up to ε^2 , to a time explicit scheme, which is consistent with the CNS equations, and in which the diffusive fluxes are approximated up to second order in space by

$$\frac{\varepsilon}{\Delta x} \left\langle vm \left(\mathcal{L}_{M_{i+\frac{1}{2}}^n}^{-1} (I - \Pi_{i+\frac{1}{2}}^n) \left(v \frac{M_{i+1}^n - M_i^n}{\Delta x} \right) - \mathcal{L}_{M_{i-\frac{1}{2}}^n}^{-1} (I - \Pi_{i-\frac{1}{2}}^n) \left(v \frac{M_i^n - M_{i-1}^n}{\Delta x} \right) \right) \right\rangle.$$

In [7], the scheme is fully discretized and implemented in the simplified case of the BGK equation.

We complete this section by a numerical illustration of the results mentioned above. In figure 3.1, we plot the heat flux profile (divided by ε) for the Sod test case, with different values of ε and for different schemes. This quantity is $\frac{1}{\varepsilon} \langle \frac{|v-u|^2}{2} (v-u) f \rangle$ in the kinetic description, and $-\kappa \partial_x T$ for the CNS equations. It is clear that the splitting scheme of [CP91] does not capture this profile for ε of the order of 10^{-4} : due to the term $e^{-\Delta t/\varepsilon}$ mentioned above, the heat flux is very small. At the contrary, our scheme gives a heat flux which is very close to that obtained with the CNS equations, as well as the modified splitting scheme.

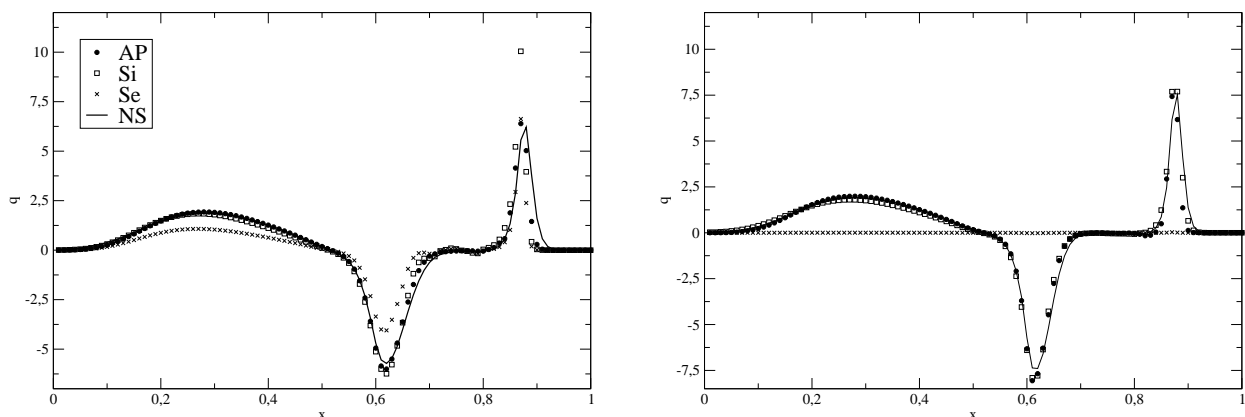


FIG. 3.1: Sod test: heat flux divided by ε as a function of $x \in [0, 1]$ for the scheme (3.10)–(3.11) (referred to as AP) and the modified splitting scheme (referred to as Si)—that both preserve the CNS asymptotics—and for a standard scheme for the CNS equations (referred to as NS), and also for the splitting scheme of [CP91] (referred to as Se). Time $t = 0.16$, and $\varepsilon = 2 \times 10^{-3}$ (left) and $\varepsilon = 2 \times 10^{-4}$ (right). The time step is $\Delta t = 2 \times 10^{-3}$.

Remark 3.1. It can be noted that to correctly capture the CNS regime, the space grid step must satisfy $\Delta x \leq \varepsilon$, and that consequently, the CFL stability condition due to the transport requires a time step $\Delta t = O(\Delta x) = O(\varepsilon)$. This means that our scheme has the same constraint as a standard explicit scheme in this regime. However, an essential difference is that our scheme is uniformly stable and accurate with respect to ε . An explicit scheme can indeed describe the CNS regime, but in the case of a variable regime (like in an atmospheric reentry problem), this scheme cannot be used up to the Euler regime. At the contrary, the splitting scheme of [CP91] can capture the Euler regime, but not the CNS regime. Up to our knowledge, our scheme is the only one that can uniformly describe all these regimes.

3.2 A numerical scheme for the linear transport equation preserving the diffusion asymptotics [8]

In this section, we summarize a joint work with M. Lemou accepted for publication in the *SIAM Journal of Scientific Computing* [8].

We have tried to apply the strategy described in the previous section to linear equations for which the suitable scaling is the diffusion one. To simplify this summary, let us consider the one-dimensional transport equation in slab geometry

$$\partial_t f + \frac{1}{\varepsilon} v \partial_x f = \frac{\sigma_S}{\varepsilon^2} (\rho - f), \quad (3.12)$$

where the density ρ is the average of f defined by $\rho = \langle f \rangle = \frac{1}{2} \int_{-1}^1 f dv$, and $v \in \Omega = [-1, 1]$ is the cosine of the angle between the propagation speed of the particles and the axis x . It can be proved that when ε tends to 0, this density converges to the solution of the diffusion equation

$$\partial_t \rho - \partial_x (\kappa \partial_x \rho) = 0, \quad (3.13)$$

where $\kappa = \frac{1}{3\sigma_S}$.

In comparison with the hyperbolic limit, the main numerical difficulty of the diffusion scaling is that the equation contains an additional stiff term: the transport term $\frac{1}{\varepsilon} v \partial_x f$. It is therefore not very clear whether the method of section 3.1 can be directly and successfully applied. However, this approach works very well, as it is explained below.

The micro-macro decomposition adapted to problem (3.12) is

$$f = \rho + \varepsilon g, \quad (3.14)$$

where g is such that $\langle g \rangle = 0$. The projection on the kernel of the collision operator is defined here by $\Pi \varphi = \langle \varphi \rangle$. Then our micro-macro formulation of equation (3.12) is

$$\partial_t \rho + \partial_x \langle v g \rangle = 0, \quad (3.15)$$

$$\partial_t g + \frac{1}{\varepsilon} (I - \Pi)(v \partial_x g) = -\frac{\sigma_S}{\varepsilon^2} g - \frac{1}{\varepsilon^2} v \partial_x \rho. \quad (3.16)$$

Using the same time and space discretization as that proposed section 3.1, we find the scheme

$$\frac{\rho_i^{n+1} - \rho_i^n}{\Delta t} + \left\langle v \frac{g_{i+\frac{1}{2}}^{n+1} - g_{i-\frac{1}{2}}^{n+1}}{\Delta x} \right\rangle = 0, \quad (3.17)$$

$$\begin{aligned} \frac{g_{i+\frac{1}{2}}^{n+1} - g_{i+\frac{1}{2}}^n}{\Delta t} + \frac{1}{\varepsilon \Delta x} (I - \Pi) \left(v^+ (g_{i+\frac{1}{2}}^n - g_{i-\frac{1}{2}}^n) + v^- (g_{i+\frac{3}{2}}^n - g_{i+\frac{1}{2}}^n) \right) \\ = -\frac{\sigma_{Si+\frac{1}{2}}}{\varepsilon^2} g_{i+\frac{1}{2}}^{n+1} - \frac{1}{\varepsilon^2} v \frac{\rho_{i+1}^n - \rho_i^n}{\Delta x}. \end{aligned} \quad (3.18)$$

It should be remarked that the stiff term $\frac{1}{\varepsilon} (I - \Pi) v \partial_x g$ in (3.16) is approximated by an explicit term in (3.18). However, the collision term $-\frac{\sigma_S}{\varepsilon^2} g$, which is stiffer, is taken implicit. It appears that this is sufficient to ensure a uniform stability with respect to ε .

Indeed, we could have proved this property in the simplified case of the telegraph equation (also called Goldstein-Taylor model). This equation reads

$$\begin{aligned}\varepsilon \partial_t u + \partial_x u &= \frac{1}{2\varepsilon}(v - u), \\ \varepsilon \partial_t v - \partial_x v &= \frac{1}{2\varepsilon}(u - v).\end{aligned}\tag{3.19}$$

It can be viewed as model (3.12) for the “velocity” set $\Omega = \{-1, 1\}$, where $\sigma_S = 1$, dv is the Lebesgue measure associated to Ω , and f is the vector (u, v) . The density is $\rho = \frac{1}{2}(u + v)$ while the “micro” part is $g = (\frac{1}{2\varepsilon}(u - v), \frac{1}{2\varepsilon}(v - u))$. Then g can be replaced by $j = \frac{1}{2\varepsilon}(u - v)$, and after simple calculations, scheme (3.17)–(3.18) applied to this equation reads

$$\frac{\rho_i^{n+1} - \rho_i^n}{\Delta t} + \frac{1}{\Delta x}(j_{i+\frac{1}{2}}^{n+1} - j_{i-\frac{1}{2}}^{n+1}) = 0,\tag{3.20}$$

$$\frac{j_{i+\frac{1}{2}}^{n+1} - j_{i+\frac{1}{2}}^n}{\Delta t} - \frac{1}{2\varepsilon\Delta x}(j_{i+\frac{3}{2}}^n - 2j_{i+\frac{1}{2}}^n + j_{i-\frac{1}{2}}^n) = -\frac{1}{\varepsilon^2}j_{i+\frac{1}{2}}^{n+1} - \frac{1}{\varepsilon^2}\frac{\rho_{i+1}^n - \rho_i^n}{\Delta x}.\tag{3.21}$$

We have then proved, by using a simple Von Neuman analysis, the following stability result.

Theorem 3.1. *Scheme (3.20)–(3.21) is l^2 -stable, i.e.*

$$\sum_i (\rho_i^n)^2 + (\varepsilon j_{i+\frac{1}{2}}^n)^2 \leq \sum_i (\rho_i^0)^2 + (\varepsilon j_{i+\frac{1}{2}}^0)^2$$

for every n , if Δt satisfies the following condition

$$\Delta t \leq \frac{1}{2} \left(\frac{\Delta x^2}{2} + \varepsilon \Delta x \right).\tag{3.22}$$

The stability condition given in this theorem is an average of the transport and diffusion CFL conditions. For large and small ε regimes, we recover these classical CFL, but with a time step which is twice as small as that given by these conditions. Note that for $\varepsilon \ll \Delta x$, the time step is no more constrained by ε , hence the uniform stability. Practically, we observed that a similar CFL condition ensures the stability for the linear transport equation.

Contrary to the work presented section 3.1, we have studied in [8] the boundary condition (BC) approximations. To simplify, the presentation below is restricted to the case of a Dirichlet BC, at the left side $x = 0$: in our micro-macro formulation, the BC on f translates to

$$\rho(t, 0) + \varepsilon g(t, 0, v) = f_L(t, v), \quad \forall v > 0.\tag{3.23}$$

The difficulty of this study relies in the fact that the BC is given only for incoming velocities: therefore, it is not possible to decouple ρ and g in this relation. Moreover, the central discretization of the flux in (3.15) requires to know g at the boundary for every velocities, while the Dirichlet BC gives a relation for positive v only. Finally, the behavior of our scheme in case of boundary layers generated by non-isotropic BC has to be investigated. We summarize below some responses to these questions.

First, we give some notations. We consider the bounded domain $[0, 1]$ discretized by the staggered grids $\{x_i = i\Delta x\}_{i=0}^N$ with $x_0 = 0$ and $x_N = 1$ that are the boundary points, and $\{x_{i+\frac{1}{2}} = (i + \frac{1}{2})\Delta x\}_{i=-1}^N$ with $x_{-\frac{1}{2}} = -\frac{1}{2}\Delta x$ and $x_{N+\frac{1}{2}} = 1 + \frac{1}{2}\Delta x$ that are two outer points. Assuming that ρ and g are known at every points at time t_n , we compute the same quantities at t_{n+1} by the following algorithm:

1. **Computing g at inner points.** Apply (3.18) to find $g_{i+\frac{1}{2}}^n$ for $i = 0$ to N only.
2. **Computing ρ at inner points.** Apply (3.17) to find ρ_i^{n+1} for $i = 1$ to $N - 1$ only.
3. **Computing ρ at boundary points.** Apply (3.17) for $i = 0$, by using the following definition for $g_{-\frac{1}{2}}^{n+1}$:

- for incoming velocities, BC (3.23) is approximated by $\rho_0^{n+1} + \frac{\varepsilon}{2}(g_{-\frac{1}{2}}^{n+1} + g_{\frac{1}{2}}^{n+1}) = f_L$, which gives the value

$$g_{-\frac{1}{2}}^{n+1} = \frac{2}{\varepsilon}(f_L - \rho_0^{n+1}) - g_{\frac{1}{2}}^{n+1}, \quad v > 0. \quad (3.24)$$

- for outgoing velocities, use the artificial Neuman BC

$$g_{-\frac{1}{2}}^{n+1}(v) = g_{\frac{1}{2}}^{n+1}(v), \quad v < 0. \quad (3.25)$$

Note that the $\frac{1}{\varepsilon}$ stiffness of (3.24) does not cause any problem, since this term is implicit. The value at the right boundary is obtained similarly.

4. **Computing g at outer points.** Since ρ_0^{n+1} is known, it is then sufficient to apply relations (3.24)–(3.25) to obtain $g_{-\frac{1}{2}}^{n+1}$.

Now, it can easily be seen that the BC obtained at the limit $\varepsilon = 0$ for ρ_0^{n+1} is

$$\rho_0^{n+1} = \frac{\int_0^1 v f_L dv}{\int_0^1 v dv}. \quad (3.26)$$

But it is known that the BC of the diffusion equation (3.13) is in fact

$$\rho(t, 0) = \lim_{y \rightarrow +\infty} \chi(t, y, v),$$

where χ is the bounded solution of the Milne problem

$$\begin{aligned} v \partial_y \chi &= \sigma_S (\langle \chi \rangle - \chi), \quad y > 0, \\ \chi(t, 0, v) &= f_L(t, v), \quad v > 0. \end{aligned} \quad (3.27)$$

When f_L is isotropic ($= \rho_L$), we find $\rho(t, 0) = \rho_L$, which is the same as the limiting numerical BC (3.26). Thus our scheme indeed captures the solution at the boundary for isotropic BC. If f_L is not isotropic, then formula (3.26) corresponds to the approximation of (3.27) obtained by equating the half-fluxes of χ in 0 and $+\infty$, which is not always a sufficient approximation.

To conclude this section, we show numerical illustrations of the previous results. Figure 3.2 shows the behavior of our method (referred to as LM in the legend) in a kinetic

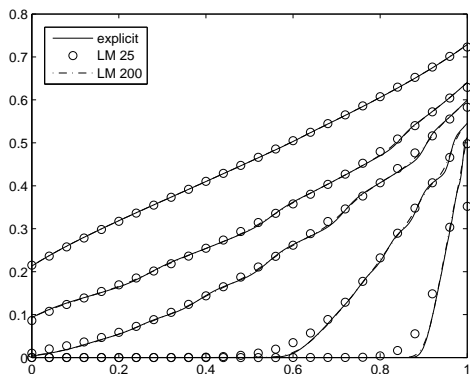


FIG. 3.2: Linear transport, kinetic regime ($\varepsilon = 1$): comparison explicit/LM schemes (LM with 25 and 200 points), at different times.

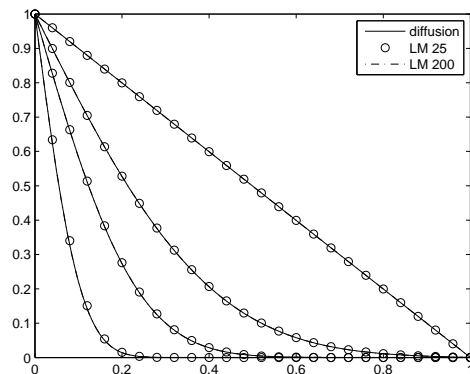


FIG. 3.3: Linear transport, diffusion regime ($\varepsilon = 10^{-8}$): comparison diffusion equation/LM scheme (25 and 200 points), at different times.

regime, while figure 3.3 shows the results obtained in the diffusion regime for different BC. The reference solutions are obtained with an explicit scheme with a very fine mesh for the kinetic regime, and with a classical approximation of the diffusion equation for the asymptotic regime.

We mention that in [8], our method is carefully compared to the methods of Klar [Kla98b] and Jin, Pareschi and Toscani [JPT00]: it globally appears that the results obtained with our approach are close to that obtained with the other methods.

3.3 Perspectives

We would like to continue these works in the following directions.

Multi-dimensional problems.

In order to fully demonstrate the efficiency of our method, it is necessary to extend it to multi-dimensional problems. The only difficulty is to obtain a suitable multi-dimensional discretization with staggered grids: in particular, an important problem is to find central differences for the gradients $\nabla_x \rho$ and $\nabla_x g$ in the linear case, or $\nabla_x M(U)$ and $\nabla_x g$ in the Boltzmann/CNS case, such that the diffusion term is well approximated by the limiting scheme. In other words, the discretized version of $\nabla_x \cdot \langle v \cdot \rangle$ applied to the discretized version of $v \cdot \nabla_x$ must be a correct approximation of the Laplace operator Δ_x . In Cartesian geometry, several simple discretizations can be tested. For an arbitrary geometry, it is attractive to consider the recent theory developed by Domelevo and Omnès [DO05]: it allows to generalize the notion of staggered grids for arbitrary meshes, and contains a discretization “in duality” of the divergence and gradient operators which seems very well suited to our problem.

Numerical boundary conditions.

The previous project will require a careful study of the discretization of the BC. We have shown in section 3.2 that, even in one dimension, this discretization is not so obvious.

This problem is still to be solved for our CNS asymptotic preserving scheme (presented section 3.1). It is not clear that the BC approximation used for the linear transport is applicable to this case.

Inversion of the collision operator.

In our approach, an important issue is to obtain an efficient inversion of the linear (or linearized) collision operator that appears in the equation for the “micro” part g . This issue is common to every AP methods (like ours or the others cited in the introduction). For the Boltzmann case, the Wild sum approach could be efficient, as it has been shown in [GPT97] or in [JP00]. Similar techniques as those we have developed for the Landau operator (see chapter 1) could also be investigated.

Mathematical analysis.

It would be interesting for the mathematical foundations of our method to extend the stability result, proved in the case of the telegraph equation, to the linear transport problem. This has already been done by Klar and Unterreiter [KU02] for a method close to that of [Kla98b] and [JPT00]. An analysis in the same spirit seems possible.

Other asymptotics.

Finally, we mention three possible extensions of our method that could be rapidly studied. First, a natural extension is to obtain a scheme for the Boltzmann equation that preserves the *incompressible* Navier-Stokes asymptotics. In this asymptotics, the distribution function is supposed to be close to an absolute Maxwellian, and the fluid limit is obtained with a diffusion scaling. Again, an AP scheme has already been obtained by Klar in [Kla99a]. We would like to prove that our scheme presented section 3.1 also allows to obtain the incompressible Navier-Stokes asymptotics.

Another extension in the diffusion limit framework is that of the “Spherical Harmonics Expansion” (S.H.E). This limit appears for kinetic models for which the collision operator makes the distribution isotropic, like in semi-conductors for instance. The equilibrium states are therefore more general than for more usual models: they are functions of the energy. The limit model is a drift-diffusion equation with a generalized gradient defined on the variables of position and energy (see Degond and Ben Abdallah [BAD96] for an introduction to these models). Our approach using the micro-macro decomposition directly applies to this problem. The only difficulty is to find a discretization of the position and energy variables that gives a correct approximation of the generalized drift-diffusion term in the limiting scheme.

Finally, we are interested in studying AP schemes for problems in which the diffusion limit is induced by the collisions at the boundary. A typical case is that of the thermal creep flow, produced in a gas confined between two plates with diffuse reflection conditions. The following chapter is devoted to such a physical situation, without studying the AP scheme problem.

Chapter 4

Models and numerical computations for a problem of microfluidics

In this chapter, we summarize several joint works with P. Degond and a few members of K. Aoki's team.

Following the recent works by Sone and co-authors [SWA96, AST⁺01], we have proposed a new system of micro-pump which is based on the thermal creep effect, as described by the kinetic theory of gases. This system is made of a curved channel along which is applied a periodic temperature field. This field induces a gas flow into the direction of the temperature gradient, without using any mechanical part, which is very interesting for obvious technological reasons. In order to demonstrate the efficiency of our device, we have proposed various modeling and numerical simulation techniques.

In section 4.1, we give some explanations on the thermal creep flow, and on its potential applications to the design of micro-pumps (called Knudsen compressors). Then in section 4.2, we present our numerical simulation method and a few numerical results. In section 4.3, we propose a macroscopic model of our problem, by using the diffusion approximation induced by the collisions with the walls, for a channel with a small width. The numerical results obtained with this model are compared to the kinetic results. Finally, we briefly describe in section 4.4 another macroscopic model obtained in the small Knudsen number limit.

4.1 Thermal creep flow and Knudsen compressors

The thermal creep flow is generated by the interaction of a gas with the boundaries, in the rarefied regime: a temperature gradient applied on the walls induces a gas flow in the direction of the gradient. This phenomenon has first been discovered by Reynolds [Rey79], then studied by Maxwell [Max79], Knudsen [Knu09], and recently, for instance, by Sone [Son66], and Ohwada, Sone and Aoki [OSA89].

Without describing these theories into details, we give below a simplified explanation of this phenomenon (taken from [Son02]). Consider a point A of the boundary (see figure 4.1) and the molecules that impact this point. Since the boundary is hotter at the right side of A than at the left side, then the molecules coming from the right have a greater average kinetic energy than those coming from the left. Consequently these molecules transfer a

momentum to A which is greater than the momentum transferred by left molecules. On the other hand, the molecules reflected diffusely on the boundary do not contribute to the tangential momentum transfer. Therefore the gas transfers a momentum to the boundary in the opposite direction to the temperature gradient direction (to say from the right to the left). Finally, since the boundary is at rest, by reaction it transfers a force to the gas directed from the left to the right. This produces a flow directed in the temperature gradient direction. This flow is called thermal creep flow.

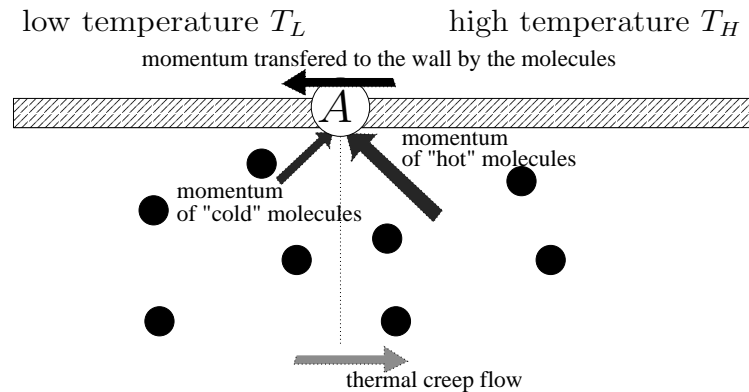


FIG. 4.1: Physical mechanism of the thermal creep flow.

This effect suggests that it is possible to create a flow in a pipe or a channel without any mechanical part. Since this idea has first been suggested by Knudsen, the devices that use the thermal creep flow are often called *Knudsen compressors*. However, this is only recently, with the development of the micro-mechanics (in particular the micro-electro-mechanical system technology, or MEMS), that it has been possible to construct Knudsen compressors sufficiently small to work with not too small pressures. For instance, for the air in atmospheric pressure, the gas is sufficiently rarefied only if the characteristic size of the device is of the order of 1 micron. Recently, different kinds of compressors have been proposed: our device uses some ideas developed by Sone, Waniguchi and Aoki [SWA96], and Sone and Sato [SS00] (see other references in [9]).

Like [SWA96], we use a cascade structure, already proposed by Knudsen: since the pumping effect induced by the thermal creep is proportional to the temperature gradient, the power of the pump is necessarily limited, except if a very strong temperature gradient is applied, which is technologically difficult. The idea is then to form a device composed of similar units connected together. Each unit is composed of a pipe divided into two parts, along which are applied two opposed temperature gradients, so that there is no gradient on average in the unit. A net flow can be generated in the device if one can find a way to avoid the compensation of the two opposed thermal creep flows generated in each unit.

In our system, this is obtained by a *geometrical effect*. As it is shown in figure 4.2, this unit has a hook shape: a temperature gradient $(T_H - T_L)/L_S$ is applied to the straight part, and an opposed gradient $(T_L - T_H)/(\pi R)$ is applied on the curved part. Due to the different geometries of the two parts, it can be expected that the two thermal creep flows will not have the same magnitude, and hence one flow should be stronger than the other. This geometry is simpler than in [SWA96] and should be easily feasible on a MEMS. Note that to limit

the computational cost of our simulations, our study has been restricted to two-dimensional plane geometries: then figure 4.2 represents a plane channel instead of a pipe.

In the studies described in the next sections, two different tests have been considered. The first one is described in figure 4.3: one unit is connected to its symmetric image so as to make a ring. This test is designed to show a steady circulating flow. The other test is designed to measure the pumping effect by using a cascade as described in figure 4.4. One unit is connected to its mirror image to form a “S” shape, then \mathcal{N} units are connected as a cascade system. The device is closed at both ends, and the pressure difference is computed at steady state.

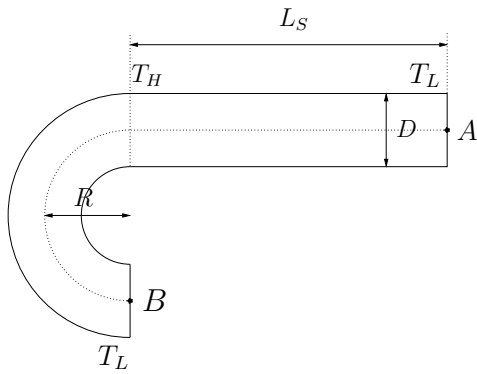


FIG. 4.2: Basic unit of our devices : a hook shaped channel.

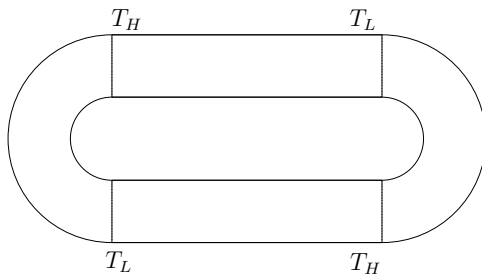


FIG. 4.3: Ring shaped channel to generate a circulating flow.

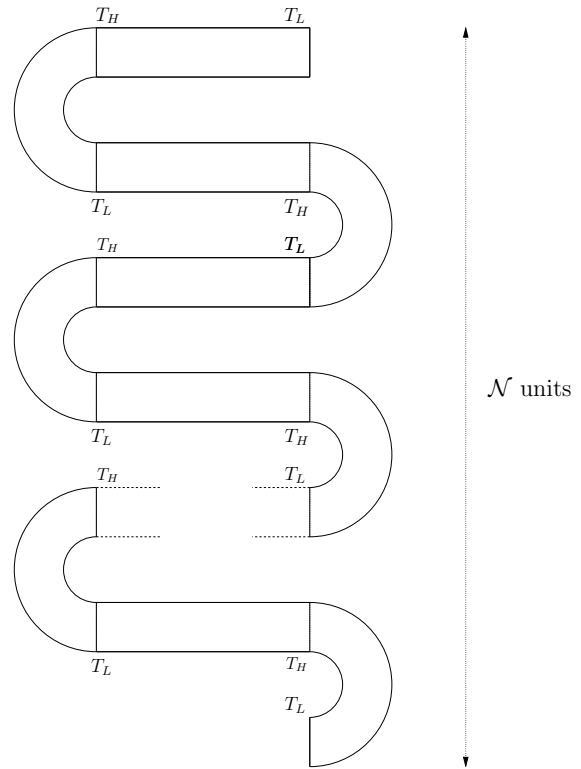


FIG. 4.4: Closed cascade device to generate a pumping effect.

4.2 Two-dimensional steady Boltzmann-BGK simulation with an implicit scheme [9, 10]

In this section, we summarize the joint work with K. Aoki and P. Degond, and submitted in 2007 [9]. We briefly detail our deterministic numerical method used to simulate the devices presented in the previous section. At the end of this section, our results are compared to these obtained with a standard stochastic simulation. These results are taken from a joint work with K. Aoki, P. Degond, M. Nishioka, and S. Takata, which has been presented in 2006 at the 25th Rarefied Gas Dynamics Symposium [10].

The Boltzmann equation is still computationally very expensive: this is why this study uses the simpler BGK model. This choice has been justified by our results (see the end of this section). In this model, the gas is described by the distribution functions $f(t, \mathbf{x}, \mathbf{v})$, where $\mathbf{x} = (x, y, z)$ is the position variable and $\mathbf{v} = (v_x, v_y, v_z)$ is the velocity variable, and the evolution of f is given by the kinetic equation

$$\partial_t f + \mathbf{v} \cdot \nabla_{\mathbf{x}} f = \frac{1}{\tau} (M[\rho, \mathbf{u}, 2RT] - f), \quad (4.1)$$

where $M[\rho, \mathbf{u}, 2RT]$ is the Maxwellian equilibrium distribution defined by $M[\rho, \mathbf{u}, 2RT] = \frac{\rho}{(2\pi RT)^{3/2}} \exp(-\frac{|\mathbf{v}-\mathbf{u}|^2}{2RT})$. The macroscopic quantities as the mass density ρ , the mean velocity \mathbf{u} , and the temperature T are defined by

$$(\rho, \rho \mathbf{u}, \frac{1}{2}\rho|\mathbf{u}|^2 + \frac{3}{2}\rho RT)(t, \mathbf{x}) = \int_{\mathbb{R}^3} (1, \mathbf{v}, \frac{1}{2}|\mathbf{v}|^2) f(t, \mathbf{x}, \mathbf{v}) d\mathbf{v}. \quad (4.2)$$

For plane flows, f is independent of z , and the complexity of (4.1) is classically reduced by the following method. We define the reduced distributions $(F, G)(t, x, y, v_x, v_y) = \int_{\mathbb{R}} (1, \frac{1}{2}v_z^2) f dv_z$, and it is easy to prove that F and G satisfy the coupled system of kinetic equations

$$\partial_t U + v \cdot \nabla_{x,y} U = Q(U), \quad (4.3)$$

where $U = (F, G)$ and $Q(U) = (\frac{1}{\tau}(\mathcal{M}[\rho, u, 2RT] - F), \frac{1}{\tau}(\frac{RT}{2}\mathcal{M}[\rho, u, 2RT] - G))$. In this equation, $v = (v_x, v_y)$ denotes the two-dimensional velocity variable. By symmetry, the macroscopic velocity \mathbf{u} has no component along z , then we note $u = (u_x, u_y)$ its component in the plane (x, y) . Finally, $\mathcal{M}[\rho, u, 2RT]$ is the Maxwellian defined by

$$\mathcal{M}[\rho, u, 2RT] = \int_{\mathbb{R}} M[\rho, \mathbf{u}, T] dv_z = \frac{\rho}{2\pi RT} \exp(-\frac{|v-u|^2}{2RT}),$$

and the macroscopic quantities can be obtained through F and G by

$$\rho = \int_{\mathbb{R}^2} F dv, \quad \rho u = \int_{\mathbb{R}^2} v F dv, \quad T = \frac{1}{\frac{3}{2}\rho R} \int_{\mathbb{R}^2} (\frac{1}{2}|v-u|^2 F + G) dv. \quad (4.4)$$

To approximate the stationary solution of the BGK equation (4.1), we have extended to the reduced system (4.3) the method that I have developed in my thesis (see [Mie00a, Mie00b]). The main ingredients of this method are:

(a) *velocity discretization*: with a Cartesian grid of N_v points $\{v_k\}$, the Maxwellian is approximated so as to preserve the conservation and entropy properties of the collision operator. The rigorous mathematical basis of this approximation have not been studied in [9], but this study can easily be made by using my previous works: existence of the approximation in [Mie00a] and [14] (see also chapter 5), and convergence in [Mie01]. In what follows, we note U_k and $Q_k(U)$ the corresponding approximations of $U(v_k)$ and $Q(U)(v_k)$.

(b) *space discretization*: with an upwind finite-volume scheme on a curvilinear structured grid of $N_{x,y}$ nodes $(x, y)_i$. To give a simple idea of this scheme, we give below the corresponding approximation in one space dimension only:

$$\partial_t U_{i,k} + v_k^+ \frac{U_{i,k} - U_{i-1,k}}{\Delta x} + v_k^- \frac{U_{i+1,k} - U_{i,k}}{\Delta x} = Q_k(U_i),$$

where v_k^\pm are the positives and negatives parts of v_k .

(c) *time discretization*: with a linearized implicit scheme which can rapidly converge to the stationary solution (with large time steps). With the previous notations, this reads

$$\frac{U_{i,k}^{n+1} - U_{i,k}^n}{\Delta t} + v_k^+ \frac{U_{i,k}^{n+1} - U_{i-1,k}^{n+1}}{\Delta x} + v_k^- \frac{U_{i+1,k}^{n+1} - U_{i,k}^{n+1}}{\Delta x} = Q_k(U_i^n) + DQ_k(U_i^n)(U_i^{n+1} - U_i^n),$$

where $DQ_k(V)$ is the derivative of Q_k computed at V .

(d) *linear solver*: the previous relation is a linear system for the unknown U^{n+1} , which is a vector of $\mathbb{R}^{2N_v N_{x,y}}$. This system can be written under the following matrix form

$$\left(\frac{I}{\Delta t} + T + R^n \right) \delta U^n = RHS^n, \quad (4.5)$$

where $\delta U^n = U^{n+1} - U^n$, I is the unit matrix, T is the matrix that discretizes the operator $v \cdot \nabla_{x,y}$, $-R^n$ is the Jacobian matrix of Q_k at U^n , and RHS^n is the matrix that discretizes $-v \cdot \nabla_{x,y} U + Q(U)$ at time n . Since the size of this system is very large, it cannot be inverted by a direct method, and the matrices cannot even be stored. It is therefore solved by an original iterative solver that makes use of the sparse structures of T (local with respect to x, y) and R^n (local with respect to v).

In comparison to [Mie00a, Mie00b], the main innovation proposed with this scheme relies on a new algorithm to treat the boundary conditions (BC) in the linear solver. Up to this work, the BC were treated explicitly, even in the implicit scheme: the coefficients corresponding to these BC in the matrix T were replaced by 0, in order to preserve the multi-diagonal

structure of the matrix. The convergence of our algorithm has been improved by using an implicit treatment of the BC that has the following advantages:

- its implementation requires only very slight modifications of the linear solver;
- the additional computational cost per iteration is neglectable;
- the induced speed-up of the global algorithm is very important.

Since a detailed explanation of this approach requires to introduce a large number of notations, we refer to [9] to limit the length of this summary.

Using this algorithm, I wrote the computational code CORBIS (COde Raréfié Bidimensionnel Implicite Stationnaire) in Fortran 90. It uses the shared memory parallel programming interface OpenMP. The results below have been obtained with 6 processors of the SGI Altix 3700 of the scientific grouping CALMIP (see <http://www.calmip.cict.fr>).

In figure 4.5, we plot the velocity field and the streamlines obtained with this code for the ring shaped channel described figure 4.3 (p.43). We observe that the flow generated by the curved boundary is stronger than that of the straight part, which remains confined in two small recirculation zones. A global net flow is indeed generated, in the indirect sense. In figure 4.6, we plot the temperature, density, pressure, and velocity fields obtained for the pumping test described figure 4.4 (p.43) with a 16 units channel. We observe the pressure difference which is obtained between both ends of the channel. In figure 4.7 is given a comparison of the results obtained with the deterministic code CORBIS to these obtained with the DSMC method (computations made by M. Nishioka in [10]) : we observe that even with the simple BGK model, the agreement with DSMC (which is supposed to approximate the Boltzmann equation) is surprisingly good, at least for 2 to 8 units channel. Note that for this last computation, the advantage of our deterministic simulation is striking: it required 7 days of computation, while the DSMC simulation took around 4 months. Finally, figure 4.8 shows the convergence speed-up obtained with the implicit treatment of the BC.

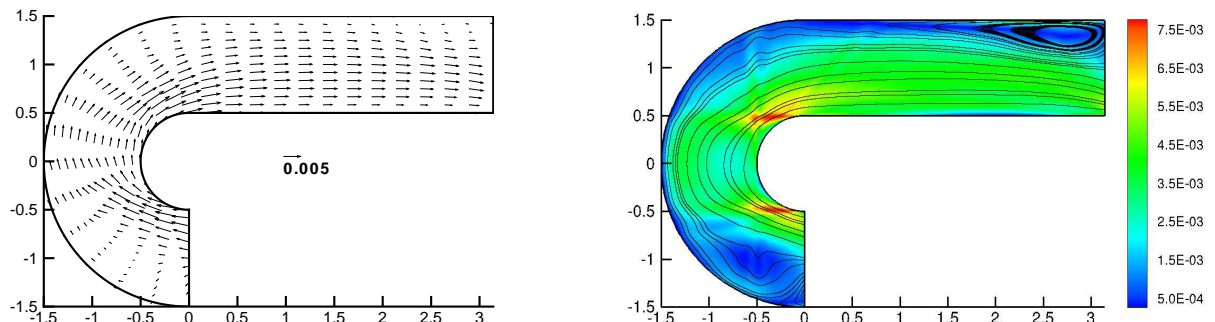


FIG. 4.5: Velocity field (left), streamlines and magnitude of the velocity field (right) in half of the ring shaped channel.

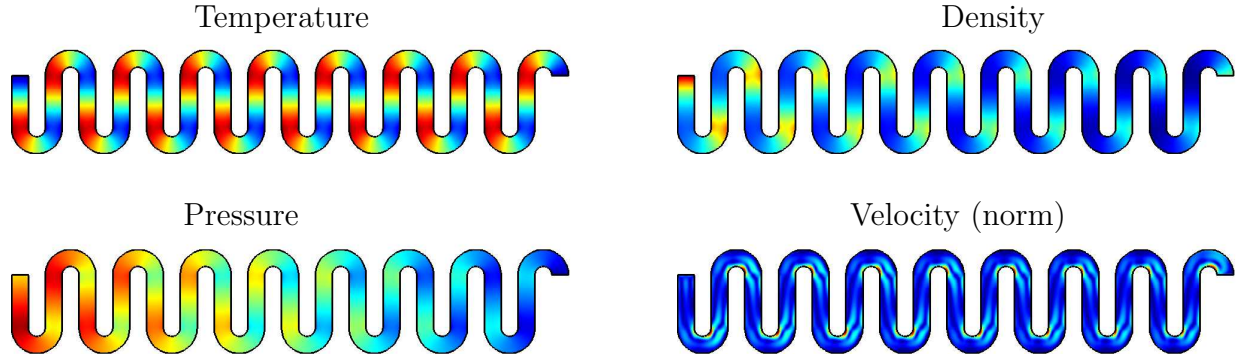


FIG. 4.6: Macroscopic fields in the 16 units pump.

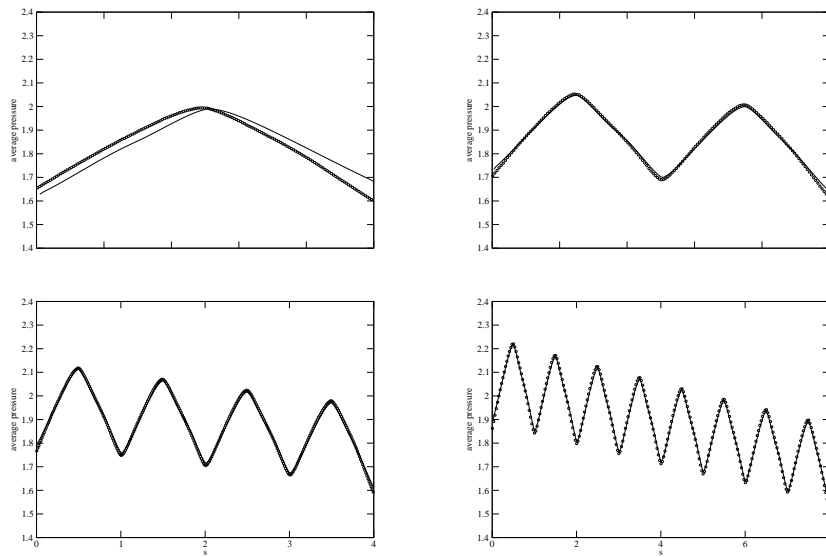


FIG. 4.7: Comparison between BGK (-) and DSMC (o): pressure (averaged in a section) along the channel, for a pump with 1, 2, 4, and 8 units.

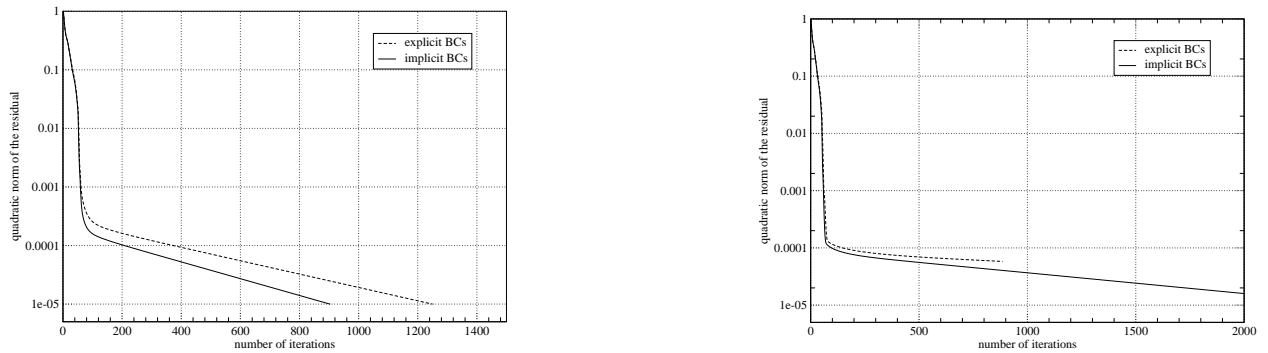


FIG. 4.8: Convergence to the stationary solution for a 8 unit (left) and a 16 unit channel (right), for our scheme with explicit and implicit BC.

4.3 Diffusion approximation induced by the collisions with the boundaries [11, 12]

Here, we present a joint work with K. Aoki, P. Degond, S. Takata, and H. Yoshida, accepted in 2007 for publication in *SIAM Multiscale Modeling & Simulation*.

In the previous study, due to the large computational cost, our simulations are limited to channels with a small number of units. A simpler modeling is then essential to study the behavior of our channel for larger numbers of units (around 100).

In this section, we obtain a macroscopic approximation of the BGK equation (4.1) for channels with a width smaller than a characteristic length (like the length of one unit). Usually, the fact that a kinetic equation can be approximated by a diffusion equation is due to the structure of the collision operator: it makes the distribution tend to an equilibrium state of zero mass flux. This implies that the asymptotic analysis must be done with a time scale sufficiently long to observe a nontrivial dynamics. In our case, this role is, somehow, played by the reflection boundary condition: the particles are diffusely reflected, at the wall temperature, with a zero average velocity. Then, when the channel is very thin, the mass flux of the gas becomes very small. This phenomenon has been studied by Babovsky [Bab86] and Babovski, Bardos and Płatkowski [BBP91] in the case of a collisionless gas, in a one-dimensional straight channel. More recently, Aoki and Degond [AD03] have extended this method to the case of a straight channel with a linear collision operator, in order to simplify the study of the Knudsen compressor proposed in [SWA96, AST⁺01]. Here, we use the same strategy applied to the curved channel. In comparison to [AD03], the differences are the followings:

- the geometry requires a study with curvilinear coordinates;
- the collision operator is nonlinear;
- we use the diffusion model for various numerical simulations: a database for the diffusion coefficients is constructed, the diffusion model is discretized, and it is compared to the kinetic simulations presented in the previous section.

In what follows, these different points are detailed.

Let us consider again the BGK equation (4.1) studied in the previous section. Here, the relaxation time is equal to $(A_c \rho)^{-1}$ where A_c is a constant. This equation is set in a plane domain Ω with a curved boundary, and of constant width D . With the coordinate system (r, s) defined in figure 4.9, the BGK equation can be written as

$$\begin{aligned} \partial_t f + (1 - \kappa r)^{-1} v_s \partial_s f + v_r \partial_r f + \kappa (1 - \kappa r)^{-1} v_r v_s \partial_{v_s} f \\ - \kappa (1 - \kappa r)^{-1} v_s^2 \partial_{v_r} f = A_c \rho (M[\rho, \mathbf{u}, 2RT] - f). \end{aligned} \quad (4.6)$$

where κ is the curvature of the median line \mathcal{C} of the channel, (v_s, v_r) are the velocities in the tangent and normal directions to \mathcal{C} in s , and $(1 - \kappa r)$ is the Jacobian of the Cartesian/cur-

vilinear transformation. The diffuse reflection condition at the walls reads

$$f = \pm \frac{1}{2\pi(RT_w)^2} \exp\left(-\frac{\mathbf{v}^2}{2RT_w}\right) \int_{v_r \gtrless 0} v_r f d\mathbf{v}, \quad \text{for } v_r \lesseqgtr 0 \quad \text{at } r = \pm \frac{D}{2}, \quad (4.7)$$

where $T_w(s)$ is the wall temperature in s .

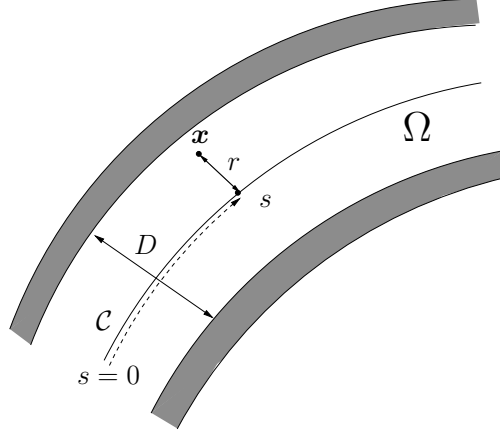


FIG. 4.9: Plane channel Ω and the associated curvilinear coordinate system.

The assumption of a small width channel is made visible with new non-dimensional variables for which equation (4.6) reads

$$\begin{aligned} \epsilon^2 \partial_t f + \epsilon(1 - \kappa r)^{-1} v_s \partial_s f + v_r \partial_r f + \kappa(1 - \kappa r)^{-1} v_r v_s \partial_{v_s} f \\ - \kappa(1 - \kappa r)^{-1} v_s^2 \partial_{v_r} f = \frac{1}{K_0} \rho(M[\rho, \mathbf{u}, T] - f), \end{aligned} \quad (4.8)$$

where K_0 is the Knudsen number, and the boundary condition is now written at $r = \pm \frac{1}{2}$. Up to some constants, this changing of variables means that we use the following time and space variables $t' = \epsilon^2 t$ and $s' = \epsilon s$, where $\epsilon = \frac{D}{L_s}$ is the ratio of the width of the channel to a characteristic length scale of variation of T_w and κ .

Integrating (4.8) on the velocity space and on a section of the channel, we find the following continuity equation:

$$\partial_t \varrho + \partial_s j = 0, \quad (4.9)$$

where

$$\varrho(s, t) = \int_{-1/2}^{1/2} \int_{\mathbb{R}^3} f(1 - \kappa r) d\mathbf{v} dr \quad \text{et} \quad j(s, t) = \frac{1}{\epsilon} \int_{-1/2}^{1/2} \int_{\mathbb{R}^3} v_s f d\mathbf{v} dr$$

are the mass density on the section, and the mass flux across the section, divided by ϵ .

First, we have found the limit of this equation as ϵ tends to 0. We mention that the results of [9] that are summarized below are formal: we do not specify any regularity assumption, nor any function space.

Theorem 4.1. (i) $f \rightarrow f_{(0)} = \rho_{(0)}(s, t)M[1, 0, T_w(s)]$ as $\epsilon \rightarrow 0$, where $\rho_{(0)}(s, t)$ is a solution of the nonlinear diffusion problem

$$\partial_t \rho_{(0)} + \partial_s j_{(1)} = 0, \quad (4.10)$$

$$j_{(1)} = \sqrt{T_w} M_P \partial_s \rho_{(0)} + \frac{\rho_{(0)}}{\sqrt{T_w}} (M_P + M_T) \partial_s T_w, \quad (4.11)$$

where M_P and M_T are nonlinear functions of $\rho_{(0)}$ defined through auxiliary linear kinetic equations (see the proof of the theorem).

(ii) The diffusion coefficient M_P is non-positive.

(iii) $\rho_{(0)}$ and $j_{(1)}$ are second order approximations of the density ϱ and current j associated to f : $\varrho - \rho_{(0)} = O(\epsilon^2)$, $j - j_{(1)} = O(\epsilon^2)$.

Sketch of the proof. Classically, we look for an approximation of the solution f under the form of a third order Hilbert expansion $f_{(0)} + \epsilon f_{(1)} + \epsilon^2 f_{(2)} + \epsilon^3 f_{(3)}$. This approximation is inserted into (4.8) and into the corresponding boundary conditions, and the nonlinear terms are expanded. Then, we use the following notations: $Q(f) = \frac{1}{K_0} \rho(M[\rho, \mathbf{u}, T] - f)$ is the collision operator and $DQ^k(f_{(0)})$ its derivatives with respect to f in $f_{(0)}$, and we introduce the the following operators:

$$\begin{aligned} \mathcal{A}^0 &= v_r \partial_r + \kappa(1 - \kappa r)^{-1} v_r v_s \partial_{v_s} - \kappa(1 - \kappa r)^{-1} v_s^2 \partial_{v_r} & L &= \mathcal{A}^0 - DQ(f_{(0)}) \\ \mathcal{A}^1 &= (1 - \kappa r)^{-1} v_s \partial_s & \mathcal{A}^2 &= \partial_t. \end{aligned}$$

It is easily found that the Hilbert approximation satisfies (4.8) up to ϵ^4 if $f_{(0)}$, $f_{(1)}$, $f_{(2)}$, and $f_{(3)}$ satisfy

$$\mathcal{A}^0 f_{(0)} = Q(f_{(0)}) \quad (4.12)$$

$$L f_{(1)} = -\mathcal{A}^1 f_{(0)} \quad (4.13)$$

$$L f_{(2)} = \frac{1}{2} D^2 Q(f_{(0)})(f_{(1)}, f_{(1)}) - \mathcal{A}^2 f_{(0)} - \mathcal{A}^1 f_{(1)} \quad (4.14)$$

$$\begin{aligned} L f_{(3)} &= D^2 Q(f_{(0)})(f_{(1)}, f_{(2)}) + \frac{1}{6} D^3 Q(f_{(0)})(f_{(1)}, f_{(1)}, f_{(1)}) \\ &\quad - \mathcal{A}^2 f_{(1)} - \mathcal{A}^1 f_{(2)}, \end{aligned} \quad (4.15)$$

and the corresponding boundary conditions.

For the zeroth order in ϵ (4.12), we assume that $f_{(0)}$ is necessarily given by

$$f_{(0)} = \rho_{(0)}(s, t) M_w, \quad (4.16)$$

where the density $\rho_{(0)}$ has to be determined, and $M_w = M[1, 0, T_w(s)]$. Note that this assumption could easily be proved by using the conservation laws and the entropy and Darrozès-Guiraud inequalities. Also note that the corresponding mass flux is necessarily zero, which a posteriori justifies our new time scale.

For the first order in ϵ (4.13), it can easily be proved that the linear operator L is invertible on the set of functions that have a zero averaged density on a section. Then, after the expansion of $\mathcal{A}^1 f_{(0)}$, we find

$$f_{(1)} = L^{-1} \left(-(1 - \kappa r)^{-1} v_s M_w \right) \partial_s \rho_{(0)} + L^{-1} \left(-(1 - \kappa r)^{-1} v_s M_w \left(\frac{\mathbf{v}^2}{T_w} - \frac{3}{2} \right) \right) \frac{\partial_s T_w}{T_w} \rho_{(0)}. \quad (4.17)$$

Now, if we assume that $f_{(0)} + \epsilon f_{(1)}$ is indeed an approximation of f , then relations (4.9), (4.16) and (4.17) are sufficient to obtain the diffusion equation (4.10)–(4.11): we find $j_{(1)} = \int_{-1/2}^{1/2} \int_{\mathbb{R}^3} v_s f_{(1)} d\mathbf{v} dr$, and the coefficients M_P and M_T are defined by

$$M_P = \int_{-1/2}^{1/2} \int_{\mathbb{R}^3} v_s \frac{1}{\sqrt{T_w}} L^{-1} \left(-(1 - \kappa r)^{-1} v_s M_w \right) d\mathbf{v} dr \quad (4.18)$$

$$M_T = \int_{-1/2}^{1/2} \int_{\mathbb{R}^3} v_s \frac{1}{\sqrt{T_w}} L^{-1} \left(-(1 - \kappa r)^{-1} v_s M_w \left(\frac{\mathbf{v}^2}{T_w} - \frac{5}{2} \right) \right) d\mathbf{v} dr. \quad (4.19)$$

The other parts of the proof are classical: $f_{(2)}$ and $f_{(3)}$ are computed like $f_{(1)}$, then we show that, by construction, the approximation $f_\epsilon = f_{(0)} + \epsilon f_{(1)} + \epsilon^2 f_{(2)} + \epsilon^3 f_{(3)}$ satisfies the same equation as f up to $O(\epsilon^2)$. This allows to prove that f_ϵ approximates f up to $O(\epsilon^2)$ (provided that the remainder can be correctly estimated), and gives points (i) and (iii) of the theorem. Point (ii) is mainly due to the fact that the operator $\frac{1}{f_{(0)}} DQ(f_{(0)})$ is non-positive self-adjoint in $L^2(\mathbb{R}^3 d\mathbf{v})$. In [9], a direct proof of this point is given. \square

In [9], the formula for M_P and M_T are a bit different: actually the inversion of L requires to solve one-dimensional stationary kinetic problems, which cannot be analytically made. These problems have then been numerically solved, in order to tabulate M_P and M_T . To do so, it must be found which independent parameters these coefficients depend on. This is why we have introduced the functions

$$\begin{aligned} \phi_P(s, r, \zeta, t) &= \frac{1}{M_w} L^{-1} \left(-(1 - \kappa r)^{-1} v_s M_w \right), \\ \phi_T(s, r, \zeta, t) &= \frac{1}{M_w} L^{-1} \left(-(1 - \kappa r)^{-1} v_s M_w \left(\frac{\mathbf{v}^2}{T_w} - \frac{5}{2} \right) \right), \end{aligned}$$

and the variable $\zeta = \mathbf{v}/\sqrt{T_w}$. Then we could have proved that ϕ_P and ϕ_T are solutions of linear problems that depend only on two parameters: the curvature κ and the local Knudsen number $K = \sqrt{T_w} K_0 / \rho_{(0)}$. The coefficients M_P and M_T then read $M_P = \int_{-1/2}^{1/2} \int_{\mathbb{R}^3} \zeta_s \phi_P E d\zeta dr$ and $M_T = \int_{-1/2}^{1/2} \int_{\mathbb{R}^3} \zeta_s \phi_T E d\zeta dr$. They depend on s only through the parameters κ and K . They could have been tabulated once for all by solving the linear problems associated to ϕ_P and ϕ_T for many values of κ and K .

Whereas the sign of M_P is easily obtained, this is more difficult for the friction coefficient $M_P + M_T$. However, such a result is interesting since it allows to obtain monotonicity properties for the pressure and density profiles. In [12], by using a linearized version of the BGK model, in a straight channel, at steady state, we could have proved the following inequalities: $M_P \leq 0$, $M_P + M_T \leq 0$, and $M_T \geq 0$. We then have proved that the pressure and temperature gradients have the same sign, while the density gradient has an opposed sign.

We have also studied the diffusion approximation when the curvature is discontinuous, since the channels presented section 4.2 have indeed a discontinuous curvature at the junction between the circular and straight parts. In this case, we can make again a Hilbert expansion,

but, separately, on left and right parts of the discontinuity (which is supposed to be located at $s = 0$). Then we obtain two diffusion equations for the densities at the left and right sides of the discontinuity, that must be coupled by two transmission conditions to get a well-posed problem. By a boundary layer analysis, we could have found the following transmission conditions

$$\rho_{(0)}|_{s=0^+} = (1 + \epsilon d)\rho_{(0)}|_{s=0^-}, \quad j_{(1)}|_{s=0^+} = j_{(1)}|_{s=0^-},$$

that are necessary to preserve the second order of the approximation. An approximated expression has been obtained for the constant d , that has been tabulated like M_P and M_T .

The numerical solving of the diffusion equation (4.10)–(4.11) at steady state has been made with a standard finite difference method. We give below two numerical results obtained with this asymptotic model. In figure 4.10, we compare the pressure profiles, computed along channels with 1, 2 and 4 units, to these obtained with the deterministic kinetic simulation described section 4.2. The agreement is clearly very good. After this validation, we can use the asymptotic model to compute the pressure profile in a channel with many units: in figure 4.11, we show the result obtained with 100 units. Between both ends, the pressure is increased by a factor 6, which is huge. Note that making such a computation with a two-dimensional kinetic code is really difficult.

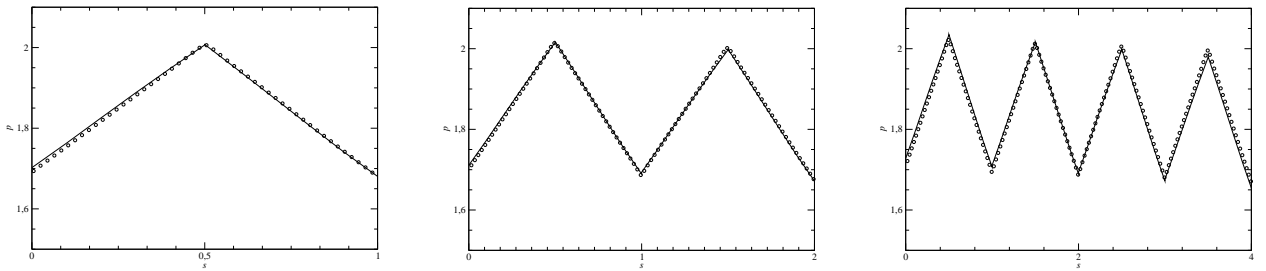


FIG. 4.10: Pressure profile along a channel with 1, 2, and 4 units: comparison between the diffusion model (-) and two-dimensional BGK simulations (o).

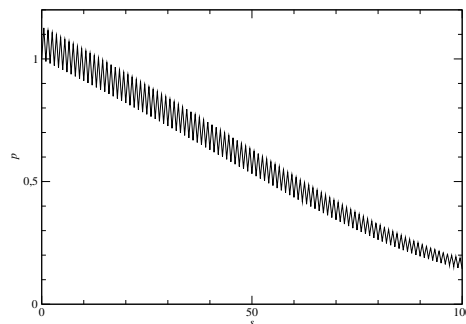


FIG. 4.11: Pressure profile along a channel with $N = 100$ units.

4.4 Approximation by a hydrodynamic model [13]

In this section, we summarize the joint work with K. Aoki, P. Degond, and C. J. T. Laneryd, presented at the 25th Rarefied Gas Dynamics Symposium [13].

In [9] and [11], we have observed that it is difficult to accurately measure the thermal creep flow as the Knudsen number is small. It is therefore natural to look for an asymptotic model of the stationary BGK equation in the small Knudsen number limit. These kinds of asymptotics have been largely investigated by Sone and his co-authors [Son02] by the Hilbert method, associated to boundary layer analyses. For the thermal creep flow, the asymptotic limit has been obtained by Sone, Aoki, Takata, Sugimoto, and Bobylev [SAT⁺96]. This limit looks like the incompressible Navier-Stokes equations, but there are a few differences: the momentum equation contains a thermal stress term, the density is not constant, and the boundary condition for the velocity is a kind of slip condition. These differences are mainly due to the finite temperature gradient assumption.

Then, with a finite-volume discretization of this model, we have made numerical simulations of the thermal creep flow, for more test cases than in the previous sections. We could have checked that there is indeed a thermal creep flow, but it disappears as the Knudsen number tends to 0. However, even at the limit Knudsen= 0, this effect still has an influence on the temperature profile: this quantity is not described by the heat equation of the incompressible Navier-Stokes model: this is an example of the (“ghost effect”) widely investigated by Sone and co-authors (see [Son02]).

4.5 Perspectives

The next step of this project will be mainly devoted to the simulation of a three-dimensional Knudsen compressor in a pipe geometry. This is physically more realistic, and the behavior of such a system may be quite different from that of the plan compressor: for instance, it has been noted in [AST⁺01] that the pipe resistance to the pressure is larger than that of a plane channel. This work will be divided into two parts.

Construction of the diffusion model.

All the calculations presented section 4.3 must be done for a three-dimensional domain Ω of constant circular section to obtain a new one-dimensional diffusion model.

Computation of the transport coefficients.

The main difficulty will be the computation of M_P and M_T : they are defined through two-dimensional auxiliary linear kinetic problems that have to be solved for a large number of values of the parameters, in order to build a database. This is a heavy computational task. We aim to modify our code CORBIS described section 4.2 to make it a linear version that could be used to make the database rapidly enough.

Chapter 5

Construction and comparisons of some simplified kinetic models

This chapter contains three works realized between 1999 and 2004. They are not related together, except that they all deal with simplified kinetic models, like the BGK model of gas dynamics and the SHE model of semi-conductor physics. Contrary to the works presented in the other chapters, these do not make part of long-term projects. This is why this chapter is not completed with a “perspective” section.

5.1 Velocity discretization of a BGK model for the polyatomic gases [14]

This section summarizes a first step towards an extension of my thesis (on the BGK equation for rarefied gases) to the case of polyatomic gases. These results have been obtained in collaboration with B. Dubroca, and have been published in 1999 in *ESAIM: proceedings* [14]. In this article, we have proposed a velocity discretization that preserves the conservation and entropy properties, for a polyatomic gas model.

We consider the following model

$$\begin{aligned}\partial_t f + v \cdot \nabla_x f &= \frac{1}{\tau}(M^{tr}[\boldsymbol{\rho}] - f), \\ \partial_t g + v \cdot \nabla_x g &= \frac{1}{\tau}(M^{int}[\boldsymbol{\rho}] - g),\end{aligned}\tag{5.1}$$

where f and g are distribution functions of mass and internal energy that depend on time t , on position $x \in \mathbb{R}^D$, and on the velocity $v \in \mathbb{R}^D$. The translational and internal equilibrium distributions are defined by

$$M^{tr}[\boldsymbol{\rho}] = M[\boldsymbol{\rho}], \quad M^{int}[\boldsymbol{\rho}] = \frac{\delta}{2}\theta M[\boldsymbol{\rho}],\tag{5.2}$$

and $M[\boldsymbol{\rho}]$ is the usual Maxwellian $M[\boldsymbol{\rho}] = \frac{\rho}{(2\pi\theta)^{D/2}} \exp(-\frac{|v-u|^2}{2\theta})$. The corresponding macroscopic quantities are the density ρ , the velocity u , and the temperature θ defined by

$$\boldsymbol{\rho} = (\rho, \rho u, \frac{1}{2}\rho|u|^2 + \frac{D+\delta}{2}\rho\theta) = \langle \mathbf{m}f + \mathbf{e}g \rangle,\tag{5.3}$$

where we use the notation $\langle \cdot \rangle = \int_{\mathbb{R}^D} \cdot dv$, and where $\mathbf{m}(v) = (1, v, \frac{1}{2}|v|^2)$ and $\mathbf{e} = (0, \dots, 0, 1)$. The parameter δ is the number of internal degrees of freedom of a molecule. This model can be deduced from the BGK model with an internal energy variable $\varepsilon(I) = I^{2/\delta}$ (which mainly represents the rotational energy of the molecule), after a classical variable reduction technique (see section 4.2 for the same technique applied to the reduction of the variable v_z). Perthame [Per99] has proved that this system has the following entropy

$$H(f, g) = \langle f \log \frac{f}{g^{\frac{\delta}{\delta+2}}} - f \rangle. \quad (5.4)$$

The local equilibria of the system can then be viewed as the minimizers of this entropy, under the constraint that moments (5.3) must be realized. Furthermore, they can be written as $M^{tr}[\boldsymbol{\rho}] = \exp(\boldsymbol{\alpha} \cdot \mathbf{m}(v))$ and $M^{int}[\boldsymbol{\rho}] = \frac{\delta}{2} [-\frac{1}{\alpha^{(D+1)}}] \exp(\boldsymbol{\alpha} \cdot \mathbf{m}(v))$ where $\boldsymbol{\alpha} = (\alpha^{(i)})_{i=0}^{D+1} = \left(\log \left(\frac{\rho}{(2\pi\theta)^{D/2}} \right) - \frac{|u|^2}{2\theta}, \frac{u}{\theta}, -\frac{1}{\theta} \right) \in \mathbb{R}^{D+2}$ is related to the Lagrange multiplier of this minimization problem.

For the velocity discretization, we use a Cartesian grid of N velocities v_k and of step Δv , and the approximations $f_{\mathcal{K}} = (f_k)_{k \in \mathcal{K}}$ and $g_{\mathcal{K}} = (g_k)_{k \in \mathcal{K}}$ of f and g on the grid. We naturally define the approximation of the macroscopic quantities (5.3) by

$$\boldsymbol{\rho}_{\mathcal{K}} = \langle \mathbf{m} f_{\mathcal{K}} + \mathbf{e} g_{\mathcal{K}} \rangle_{\mathcal{K}} = \sum_{k \in \mathcal{K}} (\mathbf{m} f_k + \mathbf{e} g_k) \Delta v^D.$$

Our problem is to find an approximation of the Maxwellians $M^{tr}[\boldsymbol{\rho}]$ and $M^{int}[\boldsymbol{\rho}]$ on the grid, so as to preserve the conservation and entropy properties at the discrete level. Following [Mie00a], we have proposed to define these approximations by the following discrete formulation of the entropy minimization problem:

$$\begin{aligned} (\mathcal{P}_{\mathcal{K}}) \quad H_{\mathcal{K}}(M_{\mathcal{K}}^{tr}[\boldsymbol{\rho}_{\mathcal{K}}], M_{\mathcal{K}}^{int}[\boldsymbol{\rho}_{\mathcal{K}}]) &= \min_{\mathcal{X}_{\boldsymbol{\rho}_{\mathcal{K}}}} \left\{ H_{\mathcal{K}}(\tilde{f}, \tilde{g}) = \langle \tilde{f} \log \frac{\tilde{f}}{\tilde{g}^{\frac{\delta}{\delta+2}}} - \tilde{f} \rangle_{\mathcal{K}} \right\}, \\ &\text{with } \mathcal{X}_{\boldsymbol{\rho}_{\mathcal{K}}} = \left\{ \tilde{f} \geq 0 \text{ and } \tilde{g} > 0 \in \mathbb{R}^N \text{ s.t. } \langle \mathbf{m} \tilde{f} + \mathbf{e} \tilde{g} \rangle_{\mathcal{K}} = \boldsymbol{\rho}_{\mathcal{K}} \right\}. \end{aligned} \quad (5.5)$$

The main contribution of this work was to determine the conditions for which this approximation is well defined. As it can be seen in the following theorem, there are two different conditions: one on the grid, and the other one on the vector $\boldsymbol{\rho}_{\mathcal{K}}$.

Theorem 5.1. *Let $\boldsymbol{\rho}_{\mathcal{K}}$ be a vector of \mathbb{R}^{D+2} . Assume that the grid \mathcal{V} is such that*

$$\{\mathbf{m}(v_k), k \in \mathcal{K}\} \text{ is of rank } D + 2, \quad (5.6)$$

then the following assertions are equivalent

- (i) *problem $(\mathcal{P}_{\mathcal{K}})$ has a unique solution $(M_{\mathcal{K}}^{tr}[\boldsymbol{\rho}_{\mathcal{K}}], M_{\mathcal{K}}^{int}[\boldsymbol{\rho}_{\mathcal{K}}])$, and there exists a unique vector $\boldsymbol{\alpha}_{\mathcal{K}} \in \mathbb{R}^{D+2}$ such that, for every $k \in \mathcal{K}$,*

$$M_k^{tr}[\boldsymbol{\rho}_{\mathcal{K}}] = \exp(\boldsymbol{\alpha}_{\mathcal{K}} \cdot \mathbf{m}(v_k)) \quad \text{and} \quad M_k^{int}[\boldsymbol{\rho}_{\mathcal{K}}] = \frac{\delta}{2} \left[-\frac{1}{\alpha_{\mathcal{K}}^{(D+1)}} \right] M_k^{tr}[\boldsymbol{\rho}_{\mathcal{K}}]; \quad (5.7)$$

(ii) $\rho_{\mathcal{K}}$ is strictly realizable on \mathcal{V} , i.e.

$$\exists(\tilde{f}, \tilde{g}) \in \mathcal{X}_{\rho_{\mathcal{K}}} \text{ such that } \tilde{f}, \tilde{g} > 0. \quad (5.8)$$

In practice, the approximations $(M_{\mathcal{K}}^{tr}[\rho_{\mathcal{K}}], M_{\mathcal{K}}^{int}[\rho_{\mathcal{K}}])$ are given by (5.7) after computing $\alpha_{\mathcal{K}}$, which is the solution of the nonlinear system of equations $\langle \mathbf{m} \exp(\alpha_{\mathcal{K}} \cdot \mathbf{m}) + \mathbf{e}^{\frac{\delta}{2}[-\frac{1}{\alpha_{\mathcal{K}}^{(D+1)}}]} \exp(\alpha_{\mathcal{K}} \cdot \mathbf{m}) \rangle_{\mathcal{K}} = \rho_{\mathcal{K}}$ given by the realizability constraints. This theorem insures the existence of $\alpha_{\mathcal{K}}$ under reasonable conditions, that are for instance satisfied if the transport operator of system (5.1) is approximated by a standard explicit scheme. Then we obtain a robust, conservative, and entropic discretization of (5.1). We conclude this section with a sketch of the proof of this theorem.

Sketch of the proof. This result is very close to that given in [Mie00a] for the monoatomic case. The demonstration consists in proving that the function

$$J(\gamma) = \langle \exp(\gamma \cdot \mathbf{m}) \rangle_{\mathcal{K}} - \gamma \cdot \rho_{\mathcal{K}} - \frac{\delta}{2} \log\left(-\frac{2}{\delta} \gamma^{(D+1)}\right) \rho_{\mathcal{K}}^{(0)},$$

deduced from the Lagrangian of problem $(\mathcal{P}_{\mathcal{K}})$, has a unique minimum in its definition domain $\mathcal{D} = \{\gamma \in \mathbb{R}^{D+2}, \gamma^{(D+1)} < 0\}$. It is sufficient to prove that J is strictly convex and coercive on \mathcal{D} .

The assumption on the grid (5.6) easily gives the strict convexity. The coercivity is a consequence of (5.6) and of the strict realizability (5.8) of $\rho_{\mathcal{K}}$. More precisely, when the behavior of J along the line $\{\gamma = \beta + s\omega, s > 0\}$ is considered, for $\beta \in \mathcal{D}$ and $\omega \in S^{D+1}$ in the case $\omega_{D+1} < 0$, then one has to compare the quantities

$$\exp(s\omega \cdot \mathbf{m}(v_k)) \quad \text{and} \quad -s\omega \cdot \rho_{\mathcal{K}}.$$

The two assumptions (5.6) and (5.8) of the theorem are used in the case $\omega \cdot \mathbf{m}(v_k) \leq 0$ for every k . Then the assumption on the grid (5.6) implies that there exists k_0 such that $\omega \cdot \mathbf{m}(v_{k_0}) < 0$, hence the assumption of strict realizability (5.8) implies $\omega \cdot \rho_{\mathcal{K}} < 0$. This means that the polynomial part of J dominates the other terms and tends indeed to infinity. The other cases do not require any assumption and are solved without any difficulty.

The explanation above is only a “directional” coercivity: that is to say J tends to infinity on every line $\{\beta + s\omega, s > 0\}$ as s grows. There remains to prove that this property implies the usual coercivity. This is in fact a general property which is stated in the following lemma:

Lemma 5.1. *Every function J defined on $\mathcal{D} = \{\gamma \in \mathbb{R}^{D+2}, \gamma^{(D+1)} < 0\}$ which is continuously differentiable, convex and coercive along every direction, is necessarily coercive in \mathcal{D} .*

In [14], we have proved this lemma by mainly using a parameterization of the level sets of J .

□

5.2 Construction and numerical approximation of BGK models with velocity dependent collision frequency [15, 16]

Here we summarize a joint work with H. Struchtrup, announced in 2004 in the 24th Rarefied Gas Dynamics Symposium [15] and published in 2004 in *Physics of Fluids* [16].

For simulating rarefied gas flows, we have proposed some BGK-like models that give correct transport coefficients in the hydrodynamic limit, by using collision frequencies that depend on the molecular velocity. These models have been numerically compared to existing models: BGK and Ellipsoidal models, and Boltzmann equation.

The BGK equation is

$$\partial_t f + v \cdot \nabla f = \nu(M - f)$$

where the Maxwellian M is defined by $M = \frac{\rho}{(2\pi RT)^{3/2}} \exp(-\frac{|v-u|^2}{2RT})$ and ρ , u , and T are the macroscopic quantities defined by the first moments of f with respect to v . In this model, the collision frequency ν depends on ρ and T only. It is well known that the viscosity and thermal conductivity coefficients μ and κ (obtained by a Chapman-Enskog expansion) are such that the Prandtl number $\text{Pr} = \frac{5}{2} R \frac{\mu}{\kappa}$ is equal to 1, while the value given by the Boltzmann equation is $\frac{2}{3}$, for monoatomic gases.

To obtain relaxation models that have proper Prandtl numbers, the general idea is to add another parameter in the model, so as to adjust μ and κ independently. In the Ellipsoidal BGK model (ES-BGK), proposed by Holway [Hol66], this is obtained by replacing the Maxwellian M by an anisotropic Gaussian. Following Struchtrup [Str97], we have considered in this work a different strategy: we preserve the isotropic structure of M , but allow for a velocity dependence of the collision frequency. More precisely, we consider the models

$$\partial_t f + v \cdot \nabla f = \nu(E - f)$$

where $\nu = \nu(\rho, T, |v - u|)$ depends on the peculiar velocity $v - u$, and E is a Maxwellian $E = \frac{\hat{\rho}}{(2\pi R\hat{T})^{3/2}} \exp(-\frac{|v-\hat{u}|^2}{2R\hat{T}})$ with parameters $\hat{\rho}$, \hat{u} , and \hat{T} that are defined so as to preserve the conservation properties. Note that these parameters are generally not equal to ρ , u and T . However, if they exist, we could have proved that this model also satisfies the entropy property.

By a Chapman-Enskog expansion, we have proved that the Prandtl number given by this model is

$$\text{Pr} = \frac{\int \frac{\eta^6}{\nu(\eta)} e^{-\eta^2} d\eta}{\int \frac{\eta^4 (\eta^2 - \frac{5}{2})^2}{\nu(\eta)} e^{-\eta^2} d\eta},$$

where $\eta = \frac{1}{\sqrt{2RT}}(v - u)$. By using functions $\nu(\eta)$ that depend on two parameters, it is therefore possible to make Pr equal to $\frac{2}{3}$. Introducing the notation $\hat{\nu} = \frac{\mu}{\rho RT} \nu$, we have constructed five simple frequencies that satisfy this constraint:

$$\begin{aligned} \hat{\nu}_1(\eta) &= 0.431587 \eta^{1.791288}, & \hat{\nu}_2(\eta) &= 0.0268351 (1 + 14.2724\eta^2), \\ \hat{\nu}_3(\eta) &= 0.0365643 (1 + 10\eta^{2.081754}), & \hat{\nu}_4(\eta) &= 0.1503991 (1 + 0.92897\eta^4), \end{aligned}$$

and $\hat{\nu}_5(\eta) = (0.2590894 \text{ if } \eta \leq 1.2, \text{ and } 0.8288236 \text{ else})$. Note that using in our model the collision frequency $\nu_{HS}(\eta) = c(e^{-\eta^2} + \frac{\sqrt{\pi}}{2}(\frac{1}{\eta} + 2\eta)\text{erf}\eta)$, obtained for the Boltzmann equation with the hard-sphere potential, does not give a correct Prandtl number.

By adapting the numerical method that I proposed in [Mie00a, Mie00b], we have tested these different models for the classical Couette (slow and fast) and stationary shock tests (Mach=1.4 to 8) from transitional regimes (Knudsen= 10^{-2}) to rarefied regimes (Knudsen=1), with comparisons to the BGK and ES-BGK models, and to the Boltzmann equation simulated by the DSMC method [Bir94]. The conclusions of this study are the followings

- for the transitional regime, as opposed to the standard BGK model, all the models that have a correct Prandtl number give results close to DSMC;
- for the rarefied regime, the results given by our BGK models with velocity dependent collision frequencies are quite different from DSMC, while BGK and ES-BGK look more accurate.

It would have been interesting to further work on the structure of the collision frequency: for instance, it seems that the functions studied in this work overestimate the collision frequency of fast particles, while that of slow particles is underestimated. However, this work has been continued by Struchtrup and Zheng [ZS05] who have combined the ES-BGK model and our idea of a velocity dependent collision frequency: the results look more correct in that case.

5.3 Numerical comparison for a kinetic equation and two Spherical Harmonics Expansion models [17]

Here, we summarize the joint work with J.-P. Bourgade and A. Mellet, and published in *Mathematical and Computer Modeling* in 2004 [17].

In semi-conductor physics, there exist some situations where the collisions of particles with the medium are mainly elastic. In this case, an asymptotic analysis shows that the diffusion approximation of the problem is a kind of intermediate between the kinetic equation and the usual drift-diffusion model. This approximation (called Spherical Harmonics Expansion, or SHE) is a diffusion equation in which the unknown is a function that depends of the particle energy.

This kind of model is often used, since it generally gives very accurate approximations of the kinetic solution. In order to improve its validity in more inelastic regimes, Degond [Deg01] has proposed a modified version called “coupled energy SHE model”. This model had never been validated before our study.

In [17], we have presented a numerical comparison of two SHE models with a linear Boltzmann equation, in a very simplified situation: one space and velocity dimension, without external field. We rapidly present below these different models and the conclusions we obtained from this study.

The kinetic model, in the diffusion scaling, is

$$\begin{aligned}\partial_t f + \frac{1}{\varepsilon} v \partial_x f &= \frac{1}{\varepsilon^2} Q(f), \quad x \in [0, 1] \\ &= \frac{1}{\varepsilon^2} (1 - \beta) Q_{el}^0(f) + \frac{1}{\varepsilon^2} \beta Q_{in}(f),\end{aligned}\tag{5.9}$$

with standard boundary conditions. The parameter β measures the relative importance of elastic and inelastic collisions, as modeled by the operators

$$Q_{el}^0(f) = \nu([f] - f), \quad \text{and} \quad Q_{in}(f) = \nu(\langle f \rangle M - f),$$

where $[f](v) = (f(v) + f(-v))/2$, $\langle f \rangle = \int_{\mathbb{R}} f(v) dv$, and $M(v) = c \exp(-\frac{m|v|^2}{2kT})$.

Since the operator Q_{in} can also be written under the form $\nu \int (f(v')M(v) - f(v)M(v')) dv'$, it can be seen that the microscopic collision mechanism of this operator consists in changing the velocity v into v' . The fact that two different SHE models can be obtained is based on the following observation: the collision can be decomposed, *by two different ways*, into an elastic collision (i.e. in which the modulus of v is conserved) and an inelastic collision. Indeed, writing $v = s\sqrt{2\mathcal{E}}$, where $\mathcal{E} = |v|^2/2$ is the energy and $s = \text{sign}(v)$ is the “direction” of v , we can decompose the collision $v \rightarrow v'$ into

$$v = (\mathcal{E}, s) \xrightarrow[\text{local}]{\text{elastic coll.}} (\mathcal{E}, s') \xrightarrow{\text{inelastic coll.}} (\mathcal{E}', s') = v',$$

or into

$$v = (\mathcal{E}, s) \xrightarrow{\text{inelastic coll.}} (\mathcal{E}', s) \xrightarrow[\text{non local}]{\text{elastic coll.}} (\mathcal{E}', s') = v',$$

where the name “local/non local” for the elastic collision highlights the fact that the collision is local or non local with respect to \mathcal{E} .

Then the first decomposition translates into Q_{in} by the following:

$$\begin{aligned}Q_{in}(f) &= \nu([f] - f) + \nu(\langle f \rangle M - [f]) \\ &= Q_{el}^0(f) + Q_{in}^0(f).\end{aligned}$$

If β is supposed to be of the order of ε^2 ($\beta = \varepsilon^2 \tilde{\beta}$), equation (5.9) reads

$$\partial_t f + \frac{1}{\varepsilon} v \partial_x f = \frac{1}{\varepsilon^2} Q_{el}^0(f) + \tilde{\beta} Q_{in}^0(f),$$

and we prove that it gives, at the limit $\varepsilon = 0$, the following SHE model:

$$\begin{aligned}\partial_t F + \partial_x J &= \nu \tilde{\beta} (\langle F \rangle M - F), \\ J &= -\frac{\sqrt{2\mathcal{E}}}{\nu} \partial_x F,\end{aligned}$$

where F depends only on \mathcal{E} . The advantage of such a model is more obvious in a multi-dimensional case, since F depends on one scalar energy variable, while f depends on a three-dimension velocity variable.

The second decomposition translates into Q_{in} by:

$$\begin{aligned} Q_{in}(f) &= \nu \left(\langle f \rangle M - 2 \int_0^\infty f(sv') dv' \right) + \nu \left(2 \int_0^\infty f(sv') dv' - f \right) \\ &= Q_{el}^1(f) + Q_{in}^1(f). \end{aligned}$$

This decomposition is then combined, in a convex way, to the previous one to obtain

$$\begin{aligned} Q &= ((1 - \alpha\beta)Q_{el}^0 + \alpha\beta Q_{el}^1) + \beta((1 - \alpha)Q_{in}^0 + \alpha Q_{in}^1), \\ &= Q_{el}^\alpha + \beta Q_{in}^\alpha. \end{aligned}$$

If we assume that the inelastic part is second order in ε , equation (5.9) reads

$$\partial_t f + \frac{1}{\varepsilon} v \partial_x f = \frac{1}{\varepsilon^2} Q_{el}^\alpha(f) + \tilde{\beta} Q_{in}^\alpha(f),$$

and we prove that it gives at the limit $\varepsilon = 0$ the coupled SHE model

$$\begin{aligned} \partial_t F + \partial_x J &= \nu \tilde{\beta} (\langle F \rangle M - F), \\ J(\mathcal{E}) &= -D_{\alpha\beta}(\mathcal{E}) \partial_x F(\mathcal{E}) - \langle \Delta_{\alpha\beta}(\mathcal{E}, \cdot) \partial_x F \rangle \end{aligned}$$

where the coefficients $D_{\alpha\beta}$ and $\Delta_{\alpha\beta}$ can be computed explicitly. Here the diffusion operator is non-local in energy, which is due to the elastic collision operator that also couples different energies.

These three models have been discretized with standard numerical methods, and several numerical tests with different collision regimes have been considered. We have observed the following facts:

- generally, the SHE and coupled SHE models are very close to Boltzmann, from elastic to inelastic regimes, even for times that are smaller than the diffusion time;
- for some regimes, the coupled SHE model is more accurate than the standard SHE model.

As a conclusion, these models give very accurate descriptions of the physical model, and their validity domain is wider than expected (since the asymptotic analysis assumes a quasi-elastic regime). However, this result should be compared to more realistic studies, with external forces, and in multi-dimensional cases.

Publications

Chapter 1.

Time Implicit schemes for the Landau equation

- [1] M. Lemou and L. Mieussens. Fast implicit schemes for the Fokker-Planck-Landau equation. *C. R. Math. Acad. Sci. Paris*, 338(10):809–814, 2004.
Note [1] announces [2].
- [2] M. Lemou and L. Mieussens. Implicit schemes for the Fokker-Planck-Landau equation. *SIAM J. Sci. Comput.*, 27(3):809–830, 2005.
- [3] M. Lemou and L. Mieussens. Time implicit schemes and fast approximations of the Fokker-Planck-Landau equation. *Bull. Inst. Math. Acad. Sin.*, 2(2):533–567, 2007.
Article [3] contains large parts of [2].

Chapter 2.

Coupling kinetic and fluid models

- [4] P. Degond, S. Jin, and L. Mieussens. A smooth transition model between kinetic and hydrodynamic equations. *J. Comput. Phys.*, 209(2):665–694, 2005.
- [5] P. Degond, G. Dimarco, and L. Mieussens. A moving interface method for dynamic kinetic-fluid coupling. *J. Comput. Phys.*, to appear.
- [6] P. Degond, J.-G. Liu, and L. Mieussens. Macroscopic fluid models with localized kinetic upscaling effects. *SIAM Multiscale Model. Simul.*, 5(3):940–979, 2006.

Chapter 3.

Asymptotic preserving numerical methods for kinetic equations in the fluid limit

- [7] M. Bennoune, M. Lemou, and L. Mieussens. Uniformly stable numerical schemes for the Boltzmann equation preserving compressible Navier-Stokes asymptotics. *J. Comput. Phys.*, to appear.
- [8] M. Lemou and L. Mieussens. A new asymptotic preserving scheme based on micro-macro formulation for linear kinetic equations in the diffusion limit. *SIAM J. Sci. Comput.*, to appear.

Chapter 4.**Models and numerical computations for a problem of microfluidics**

- [9] K. Aoki, P. Degond, and L. Mieussens. Numerical simulations of rarefied gases in curved channels: thermal creep, circulating flow, and pumping effect. Submitted (2007).
- [10] K. Aoki, P. Degond, L. Mieussens, M. Nishioka, and S. Takata. Numerical simulation of a Knudsen pump using the effect of curvature of the channel. In M. S. Ivanov and A. K. Rebrov, editors, *Rarefied Gas Dynamics*, pages 1079–1084. Siberian Branch of the Russian Academy of Sciences, Novosibirsk, 2007.
- [11] K. Aoki, P. Degond, L. Mieussens, S. Takata, and H. Yoshida. A diffusion model for rarefied flows in curved channels. *SIAM Multiscale Model. Simul.*, to appear.
- [12] L. Mieussens. A note on pressure and density profiles of flows induced by the thermal creep in straight channels.
This note has not been submitted for publication.
- [13] C. J. T. Laneryd, K. Aoki, P. Degond, and L. Mieussens. Thermal creep of a slightly rarefied gas through a channel with curved boundary. In M. S. Ivanov and A. K. Rebrov, editors, *Rarefied Gas Dynamics*, pages 1111-1116. Siberian Branch of the Russian Academy of Sciences, Novosibirsk, 2007.

Chapter 5.**Construction and comparisons of some simplified kinetic models**

- [14] B. Dubroca and L. Mieussens. A conservative and entropic discrete-velocity model for rarefied polyatomic gases. In *CEMRACS 1999 (Orsay)*, volume 10 of *ESAIM Proc.*, pages 127–139 (electronic). Soc. Math. Appl. Indust., Paris, 1999.
- [15] L. Mieussens and H. Struchtrup. Numerical solutions for the BGK-model with velocity-dependent collision frequency. *Rarefied Gas Dynamics: 23rd International Symposium, AIP Conference Proceedings*, volume 663, pages 320–327, 2003.
Article [15] announces [16].
- [16] L. Mieussens and H. Struchtrup. Numerical comparison of Bathnagar–Gross–Krook models with proper Prandtl number. *Physics of Fluids*, 16(8):2797–2813, 2004.
- [17] J.-P. Bourgade, A. Mellet, and L. Mieussens. Numerical comparison between two spherical harmonics expansion models and a kinetic equation. *Math. Comput. Modelling*, 40(7-8):777–795, 2004.

Bibliography

- [AD03] K. Aoki and P. Degond. Homogenization of a flow in a periodic channel of small section. *Multiscale Model. Simul.*, 1(2):304–334, 2003.
- [AL03] X. Antoine and M. Lemou. Wavelet approximation of a collision operator in kinetic theory. *C.R Acad. Sci., Ser. I(337)*, 2003.
- [AST⁺01] K. Aoki, Y. Sone, S. Takata, K. Takahashi, and G. A. Bird. One-way flow of a rarefied gas induced in a circular pipe with a periodic temperature distribution. In Timothy J. Bartel and Michael A. Gallis, editors, *Rarefied gas dynamics, Vol 1: 22nd International Symposium*, volume 585, pages 940–947. AIP, 2001.
- [Bab86] H. Babovsky. On Knudsen flows within thin tubes. *J. Statist. Phys.*, 44(5-6):865–878, 1986.
- [BAD96] N. Ben Abdallah and P. Degond. On a hierarchy of macroscopic models for semiconductors. *J. Math. Phys.*, 37(7):3306–3333, 1996.
- [BBP91] H. Babovsky, C. Bardos, and T. Płatkowski. Diffusion approximation for a Knudsen gas in a thin domain with accommodation on the boundary. *Asymptotic Anal.*, 3(4):265–289, 1991.
- [BC99] C. Buet and S. Cordier. Numerical analysis of conservative and entropy schemes for the Fokker-Planck-Landau equation. *SIAM J. Numer. Anal.*, 36(3):953–973, 1999.
- [BC02] C. Buet and S. Cordier. Numerical analysis of the isotropic Fokker-Planck-Landau equation. *J. Comput. Phys.*, 179(1):43–67, 2002.
- [BGL91] C. Bardos, F. Golse, and D. Levermore. Fluid dynamic limits of kinetic equations. I. Formal derivations. *J. Statist. Phys.*, 63(1-2):323–344, 1991.
- [Bir94] G.A. Bird. *Molecular Gas Dynamics and the Direct Simulation of Gas Flows*. Oxford Science Publications, 1994.
- [BKP87] Y. A. Berezin, V. N. Khudick, and M. S. Pekker. Conservative finite-difference schemes for the Fokker-Planck equation not violating the law of an increasing entropy. *J. Comput. Phys.*, 69(1):163–174, 1987.

- [BM02] G. Bal and Y. Maday. Coupling of transport and diffusion models in linear transport theory. *M2AN Math. Model. Numer. Anal.*, 36(1):69–86, 2002.
- [BTT96] J.-F. Bourgat, P. Le Tallec, and M. D. Tidriri. Coupling Boltzmann and Navier-Stokes equations by friction. *J. Comput. Phys.*, 127:227–245, 1996.
- [Caf80] R. E. Caflisch. The fluid dynamic limit of the nonlinear Boltzmann equation. *Comm. Pure Appl. Math.*, 33(5):651–666, 1980.
- [CBKM00] L. Chacón, D. C. Barnes, D. A. Knoll, and G. H. Miley. An implicit energy-conservative 2D Fokker-Planck algorithm. II. Jacobian-free Newton-Krylov solver. *J. Comput. Phys.*, 157(2):654–682, 2000.
- [CP91] F. Coron and B. Perthame. Numerical Passage from Kinetic to Fluid Equations. *SIAM J. Numer. Anal.*, 28(1):26–42, 1991.
- [Deg01] P. Degond. An infinite system of diffusion equations arising in transport theory: the coupled spherical harmonics expansion model. *Math. Models Methods Appl. Sci.*, 11(5):903–932, 2001.
- [DJ05] P. Degond and S. Jin. A smooth transition model between kinetic and diffusion equations. *SIAM J. Numer. Anal.*, 42(6):2671–2687, 2005.
- [DL01] P. Degond and M. Lemou. On the viscosity and thermal conduction of fluids with multivalued internal energy. *Eur. J. Mech. B Fluids*, 20(2):303–327, 2001.
- [DO05] K. Domelevo and P. Omnes. A finite volume method for the Laplace equation on almost arbitrary two-dimensional grids. *M2AN Math. Model. Numer. Anal.*, 39(6):1203–1249, 2005.
- [DP] G. Dimarco and L. Pareschi. Hybrid multiscale methods II. Kinetic Equations. submitted.
- [DS99] P. Degond and C. Schmeiser. Kinetic boundary layers and fluid-kinetic coupling in semiconductors. *Transport Theory Statist. Phys.*, 28(1):31–55, 1999.
- [GJL03] F. Golse, S. Jin, and C. D. Levermore. A domain decomposition analysis for a two-scale linear transport problem. *M2AN Math. Model. Numer. Anal.*, 37(6):869–892, 2003.
- [GPT97] E. Gabetta, L. Pareschi, and G. Toscani. Relaxation Schemes for Non Linear Kinetic Equations. *SIAM J. Numer. Anal.*, 34(6):2168–2194, 1997.
- [Hol66] L. H. Holway. Kinetic theory of shock structure using an ellipsoidal distribution function. In New York Academic Press, editor, *Rarefied Gas Dynamics, Vol. 1 (Proc. Fourth Internat. Sympos. Univ. Toronto, 1964)*, pages 193–215, 1966.
- [Jin99] S. Jin. Efficient asymptotic-preserving (AP) schemes for some multiscale kinetic equations. *SIAM J. Sci. Comput.*, 21(2):441–454, 1999.

- [JP00] S. Jin and L. Pareschi. Discretization of the multiscale semiconductor Boltzmann equation by diffusive relaxation schemes. *J. Comput. Phys.*, 161(1):312–330, 2000.
- [JP01] S. Jin and L. Pareschi. Asymptotic-preserving (AP) schemes for multiscale kinetic equations: a unified approach. In *Hyperbolic problems: theory, numerics, applications, Vol. I, II (Magdeburg, 2000)*, volume 141 of *Internat. Ser. Numer. Math.*, 140, pages 573–582. Birkhäuser, Basel, 2001.
- [JPT98] S. Jin, L. Pareschi, and G. Toscani. Diffusive relaxation schemes for multiscale discrete-velocity kinetic equations. *SIAM J. Numer. Anal.*, 35(6):2405–2439, 1998.
- [JPT00] S. Jin, L. Pareschi, and G. Toscani. Uniformly accurate diffusive relaxation schemes for multiscale transport equations. *SIAM J. Numer. Anal.*, 38(3):913–936, 2000.
- [Kla98a] A. Klar. Asymptotic-induced domain decomposition methods for kinetic and drift diffusion semiconductor equations. *SIAM J. Sci. Comput.*, 19(6):2032–2050, 1998.
- [Kla98b] A. Klar. An asymptotic-induced scheme for nonstationary transport equations in the diffusive limit. *SIAM J. Numer. Anal.*, 35(3):1073–1094, 1998.
- [Kla99a] A. Klar. An asymptotic preserving numerical scheme for kinetic equations in the low Mach number limit. *SIAM J. Numer. Anal.*, 36(5):1507–1527, 1999.
- [Kla99b] A. Klar. A numerical method for kinetic semiconductor equations in the drift-diffusion limit. *SIAM J. Sci. Comput.*, 20(5):1696–1712, 1999.
- [KNS00] A. Klar, H. Neunzert, and J. Struckmeier. Transition from kinetic theory to macroscopic fluid equations: a problem for domain decomposition and a source for new algorithms. *Transport Theory Statist. Phys.*, 29(1-2):93–106, 2000.
- [Knu09] M. Knudsen. Eine revision der gleichgewichtsbedingung der gase. *Annalen der Physik*, 336(1):205–229, 1909.
- [KS98] A. Klar and N. Siedow. Boundary layers and domain decomposition for radiative heat transfer and diffusion equations: applications to glass manufacturing process. *European J. Appl. Math.*, 9(4):351–372, 1998.
- [KU02] A. Klar and A. Unterreiter. Uniform stability of a finite difference scheme for transport equations in diffusive regimes. *SIAM J. Numer. Anal.*, 40(3):891–913, 2002.
- [Lem98] M. Lemou. Multipole expansions for the Fokker-Planck-Landau operator. *Numer. Math.*, 78(4):597–618, 1998.

- [Lev96] C.D. Levermore. Moment Closure Hierarchies for Kinetic Theories. *J. Stat. Phys.*, **83**:1021–1065, 1996.
- [Max79] J. C. Maxwell. On stresses in rarified gases arising from inequalities of temperature. *Philosophical Transactions of the Royal Society of London*, 170:231–256, 1879.
- [MD94] J. C. Mandal and S. M. Deshpande. Kinetic flux vector splitting for Euler equations. *Comput. & Fluids*, 23(2):447–478, 1994.
- [Mie00a] L. Mieussens. Discrete Velocity Model and Implicit Scheme for the BGK Equation of Rarefied Gas Dynamics. *Math. Models and Meth. in Appl. Sci.*, 8(10):1121–1149, 2000.
- [Mie00b] L. Mieussens. Discrete-velocity models and numerical schemes for the Boltzmann-BGK equation in plane and axisymmetric geometries. *J. Comput. Phys.*, 162:429–466, 2000.
- [Mie01] L. Mieussens. Convergence of a discrete-velocity model for the Boltzmann-BGK equation. *Comput. Math. Appl.*, 41(1-2):83–96, 2001.
- [OSA89] T. Ohwada, Y. Sone, and K. Aoki. Numerical analysis of the shear and thermal creep flows of a rarefied gas over a plane wall on the basis of the linearized boltzmann equation for hard-sphere molecules. *Phys. Fluids A*, 1:1588–1599, 1989.
- [Per99] B. Perthame. An introduction to kinetic schemes for gas dynamics. In *An introduction to recent developments in theory and numerics for conservation laws (Freiburg/Littenweiler, 1997)*, volume 5 of *Lect. Notes Comput. Sci. Eng.*, pages 1–27. Springer, Berlin, 1999.
- [PRT00] L. Pareschi, G. Russo, and G. Toscani. Fast spectral methods for the Fokker-Planck-Landau collision operator. *J. Comput. Phys.*, 165(1):216–236, 2000.
- [Qiu93] Y. Qiu. *Étude des équations d’Euler et de Boltzmann et de leur couplage. Application à la simulation numérique d’écoulements hypersoniques de gaz raréfiés*. Institut National de Recherche en Informatique et en Automatique (INRIA), Rocquencourt, 1993. Thèse, Université Paris VI, Paris, 1993.
- [Rey79] O. Reynolds. On certain dimensional properties of matter in the gaseous state. Part I and II. *Philosophical Transactions of the Royal Society of London*, 170:727–845, 1879.
- [Saa03] Y. Saad. *Iterative methods for sparse linear systems*. Society for Industrial and Applied Mathematics, Philadelphia, PA, second edition, 2003.
- [SAT+96] Y. Sone, K. Aoki, S. Takata, H. Sugimoto, and A. V. Bobylev. Inappropriateness of the heat-conduction equation for description of a temperature field

- of a stationary gas in the continuum limit: Examination by asymptotic analysis and numerical computation of the Boltzmann equation. *Physics of Fluids*, 8(2):628–638, 1996.
- [Sch96] J. Schneider. Direct coupling of fluid and kinetic equations. *Transport Theory Statist. Phys.*, 25(6):681–698, 1996.
- [Son66] Y. Sone. Thermal creep in rarefied gas. *J. Phys. Soc. Jpn.*, 21:1836–1837, 1966.
- [Son02] Y. Sone. *Kinetic theory and fluid dynamics*. Modeling and Simulation in Science, Engineering and Technology. Birkhäuser Boston Inc., Boston, MA, 2002.
- [SS00] Y. Sone and K. Sato. Demonstration of a one-way flow of a rarefied gas induced through a pipe without average pressure and temperature gradients. *Physics of Fluids*, 12(7):1864–1868, 2000.
- [Str97] H. Struchtrup. The BGK-Model with Velocity-Dependent Collision Frequency. *Continuum Mech. Thermodyn.*, 9:23–31, 1997.
- [SWA96] Y. Sone, Y. Waniguchi, and K. Aoki. One-way flow of a rarefied gas induced in a channel with a periodic temperature distribution. *Physics of Fluids*, 8(8):2227–2235, 1996.
- [TM97] P. Le Tallec and F. Mallinger. Coupling Boltzmann and Navier-Stokes equations by half fluxes. 136:51–67, 1997.
- [ZS05] Y. Zheng and H. Struchtrup. Ellipsoidal statistical Bhatnagar-Gross-Krook model with velocity-dependent collision frequency. *Phys. Fluids*, 17(12):127103, 17, 2005.